HETEROGENEITY IN TWO-COMPONENT SIGNALING SYSTEMS WITHIN DIFFERENT STRAINS OF INFLAMMATORY BOWEL DISEASE ASSOCIATED *ESCHERICHIA COLI.*

By: Adam Khan,
Honours Bachelor of Science, 2016 University of Toronto

A thesis
presented to Ryerson University in partial fulfillment of the requirements for the degree of
Master of Science
in the program of Molecular Science

Toronto, Ontario, Canada, 2019

AUTHOR'S DECLARATION FOR ELECTRONIC SUBMISSION OF A THESIS

I hereby declare that I am the sole author of this thesis. This is a true copy of the thesis, including any required final revisions, as accepted by my examiners.

I authorize Ryerson University to lend this thesis to other institutions or individuals for the purpose of scholarly research.

I further authorize Ryerson University to reproduce this thesis by photocopying or by other means, in total or in part, at the request of other institutions or individuals for the purpose of scholarly research.

I understand that my thesis may be made electronically available to the public.

Abstract

Heterogeneity in two-component signaling systems within different strains of inflammatory bowel disease associated *Escherichia coli.*

Adam Khan, Master of Science, Molecular Science, Ryerson University, 2019

Resistance to host-defense peptides is a critical feature of many pathogens. Previous work in the McPhee lab has demonstrated that different strains of inflammatory bowel disease-associated *Escherichia coli* exhibit diverse resistance to host defense peptides. The PhoPQ two-component system is a well-characterized signaling pathway that regulates the expression of genes involved in resistance to these peptides. We hypothesize that strains have an altered capacity to signal through this system, resulting in different resistance profiles. We created a promoter-GFP fusion of two PhoPQ regulated genes, *pmrD* and *ompT,* to monitor PhoPQ signaling in eight clinical isolates. Our data shows that strains have robust differences in signaling when cultured identical conditions, supporting our hypothesis. Further, our signaling match polymyxin B resistance when using the same isolates and conditions. Our data strongly suggests that strains have an altered potential to respond to environmental signals, ultimately resulting in a broad level of resistance phenotypes.

Table of Contents

List of Tables

List of Figures

List of Abbreviations

A/E = attaching and effacing
AIEC = adherent-invasive *E. coli*
BP = base pair
CA = catalytic and ATP-binding
CAMP = cationic antimicrobial peptides
CD = Crohn's disease
CEACAM = carcinoembryonic antigen–related cell adhesion molecules
CFU = colony forming unit
DHp = dimerization and histidine phosphotransfer
DSS = dextran sulphate sodium
DNA = deoxyribonucleic acid
EA = ethanolamine
EHEC = enterohemorrhagic *E. coli*
EPEC = enteropathogenic *E. coli*
ETEC = enterotoxigenic *E. coli*
FD = fast digest
Fe = iron
GFP = green fluorescent protein
GI = gastrointestinal tract
GPL = glycerophospholipids
GWAS = genome wide association study
hBD = human beta defensin
HA = hemagglutinin
HDP = host defense peptide
HF = high-fidelity
HK = histidine kinase
Hpt = histidine phosphotransferase
HNP = human neutrophil peptide/protein
IBD = inflammatory bowel disease
IBDEC = IBD-associated *E. coli*
ICP = inductively coupled plasma
Ig = immunoglobulin
IL = interleukin
INF-γ = interferon gamma
IS = insertion sequence
KB = kilobase
LB = lysogeny broth
LEE = locus of enterocyte effacement
LPS = lipopolysaccharide
MCS = multiple cloning sites
MDP = muramyl dipeptide
Mg = magnesium
MQ = milli Q
NK = natural killer cell
NOD = nucleotide oligomerization domain
OCCC = Ontario Crohn's and Colitis Cohort
OD = optical density
PBS = phosphate buffer saline
PCR = polymerase chain reaction
PD = periplasmic domain
PMB = polymyxin B
REC = receiver domain
RFU = relative fluorescence units
RR = response regulator
SAK = staphylokinase
SCFA = short chain fatty acid
SNP = single nucleotide polymorphism
S.O.C. = super optimal broth with catabolite repression
SOE-PCR = single overlap extension polymerase chain reaction
T3SS = type III secretion system
TCS = two-component system
Tir = translocated intimin receptor
TNF = tumor necrosis factor
UC = ulcerative colitis
UPEC = uropathogenic *E. coli*
UTI = urinary tract infection
UV = ultraviolet
WT = wild-type

1. Introduction

1.1. Inflammatory bowel disease

Inflammatory bowel disease (IBD) is a family of disorders that results in chronic inflammation of the gastrointestinal (GI) tract[7]. The disease is further categorized into one of two conditions: ulcerative colitis (UC), which affects the colon, and Crohn's disease (CD), which is primarily localized to the ileum and caecum[8]. The onset of either condition results in symptoms such as abdominal pain, bloody diarrhea, fatigue, fever and decreased appetite[7,8]. The nature of IBD results in a cyclic pattern of disease flares followed by times of remission. This pattern, if not treated appropriately, can result in permanent damage to the intestine[9]. While no cure of the disease exists, the current treatment methods include reducing the symptoms during flares through the use of biological drugs, antibiotics, steroids, anti-inflammatories and surgery when drug therapy is unsuccessful[7,10]. The former of the treatment options has had an enormous impact on patients living with IBD, as this surgery has demonstrated the ability to heal the mucosa and substantially decrease disease progression or the further need for hospitalization[10]. Two anti–tumor necrosis factor (anti-TNF) drugs called infliximab and adalimumab are used as the most common methods of biologic therapy[7,9,10]. While the introduction and success of these drugs has been remarkable, two fundamental problems exist. 1) Approximately one third of patients do not respond to these drugs, and up to 40% of initial responders lose their response over time[9]. 2) Biologic drugs are not a cure for IBD; therefore, the continuous prescription of this medication is required to reduce the chance of flares and progression of the disease, which has a large financial burden[10].

While IBD is a global burden with a prevalence rate of 0.5% (as of 2015) per general population of the Western world (including North America, Europe, New Zealand and Australia)[11], Canada is in the top 20% for incidence rate for both UC and CD, corresponding to a 0.67% rate per general population[7]. This incidence rate, which translated to approximately 230,000 cases of both UC and CD in 2012, not only has huge implications on the quality of life for patients but is also a tremendous financial burden on the healthcare system. Direct medical costs such as hospitalization, surgery, medications, laboratory tests and procedures for the treatment of IBD in Canada accounted for upwards of $1.2 billion in 2012. Of this, the majority

of the funds were allocated to drug cost and inpatient hospitalization[7]. IBD is a complex and multifaceted disorder that contains a number of factors which influence the disease state[11]. The three predominate factors that influence the development of the disease are environmental exposures, genetics and the gut microbiota population. Therefore, in order to fully recognize the intricacies of the disease, comprehensive understanding of all three primary factors is needed to successfully mitigate the financial and personal burden of IBD. As a result, the remaining portion of this section will be devoted to discussing each of the three factors individually.

1.1.1. Environmental contribution

Environmental exposures play a significant role in the onset of IBD. IBD is most prevalent in developed countries such as Canada and the United States[7,12,13]. This trend of higher IBD rates in developed countries is supported by parallel increases of IBD and industrialization of developing countries[11,12]. Since the relationship between smoking and IBD was first reported by Harries *et al*., there has been extensive work on this interaction[15]. Interestingly, while there seems to be a causal relationship between smoking and IBD, the effect of smoking on the disease state, whether it is direct or inverse, depends on the condition being discussed[11,12,14]. There is a direct causal relationship of smoking on CD. Smokers who have active CD have a dysbiosis of the gut microbiota that could be a potential source of this causal relationship[11,12,16]. In contrast, smoking appears to have a protective role in relation to UC, as most of the patients are either non-smokers or ex-smokers[11,12,17]. Further, the relationship between diet and IBD has also been extensively studied. The results from a variety of studies consistently demonstrate in showing that a high-fat diet, predominately from red-meat, margarine and fish was associated with developing IBD, while diets rich in carbohydrates seem to have a negative effect on IBD[11,12]. Together, these results support the complex and multifactorial nature of IBD causation.

1.1.2. Host genetics

Canada continues to have one of the highest rates of IBD globally due to rising pediatric IBD cases[67-69]. The Ontario Crohn's and Colitis Cohort (OCCC) completes population-based surveillance programs that monitor cases of IBD throughout the province. Data from 1991 –

2008 showed increasing trends of pediatric IBD cases in children younger than the age of 10 years old while rates for adults and the elderly remained relatively stable[69]. Age of onset produces distinct disease phenotypes and different responses to genetic predisposition. Patients with early-onset CD (characterized by onset of disease under the age of 5) show more colonic involvement and rectal bleeding than onset of CD in children from the ages of 6-17, who display majority ileocolonic disease localization and more diverse range of symptoms[70]. Furthermore, genetic predisposition has more of a pronounced impact on pediatric onset patients, who exhibit a higher propensity for mutations in genes associated with the onset of IBD[71].

Several large-scale genome-wide association studies (GWAS) have been completed that aim to find genetic differences between healthy individuals and patients with IBD. These studies have been very successful in identifying genes associated with disease predisposition, and close to 200 genes are currently known to predispose individuals to UC and/or CD. Of these, single-nucleotide polymorphisms (SNPs) in genes that confer strongest association with IBD are *NOD2*, *IL23R*, and *ATG16L1*[11,18-22]. NOD2 is an intracellular receptor found on macrophages, dendritic cells, and Paneth cells that is able to sense muramyl dipeptide (MDP), a common component of both gram-positive and gram-negative peptidoglycan[57,72]. This detection results in the production of NF-κB, a transcription factor that is crucial in propagating an immune response. Ogura and colleagues found that if the NOD2 protein is truncated via a cytosine insertion at nucleotide 3020 resulting in a premature stop codon, induction of NF-κB is lost. This frameshift mutation in *NOD2* is associated with a susceptibility to CD[20]. IL23R is an immune receptor that is highly expressed on activated Th17 cells and natural killer (NK) cells. Downstream effects of inducing this receptor includes production of cytokines IL-17A, IL- 17F, IL-22 and IL-21, and proliferation and survival of Th17 cells. R381Q, an IL23R variant, seems to have a protective effect against CD and IBD. In 2011, Pidasheva *et al*. found evidence that R381Q achieves this protective outcome by diminishing signaling through the JAK/STAT pathway[21].

Lastly, ATG16L1 is a protein that is involved in an important cellular recycling process called autophagy that occurs by fusion of a double-membraned vesicle containing cytoplasmic cargo with a lysosome. A Thr300Ala SNP in the *ATG16L1* increases the sensitization of

ATG16L1 to capase-3 mediated cleavage, ultimately diminishing autophagy. This weakened response was correlated with a defect in the removal of ileal pathogen *Yersinia enterocolitica* and also resulted in higher induction of pro-inflammatory cytokines[46]. Mice raised with hypomorphic ATG16L1 display a defect in Paneth and epithelial cells. Paneth cells are specialized cells part of the ileal epithelium layer that serve a main function of secreting granules with antimicrobial peptides. The hypomorphic ATG16L1 protein in mice show distinct irregularities in the granular exocytic pathway and an increase in cytoplasmic vesicles. Interestingly, similar phenotypic defects have been reported in the Paneth cells of CD patients positive with the *ATG16L1* risk allele[58,59]. Mutation in ATG16L1 is also shown to affect the overall transcriptional profile of the cells, most importantly resulting in an increase of lipid metabolism genes and pro-inflammatory cytokines. Following LPS stimulation, NOD2 recruits ATG16L1 to the bacterial plasma membrane where the process of autophagy begins. Plantinga and colleagues (2011) showed that loss of autophagy due to polymorphism in *ATG16L1* increases the production of pro-inflammatory cytokines IL-1β and IL-6 after NOD2 stimulation, linking the chronic inflammation phenotype seen in Crohn's disease patients[73,78]. Therefore, genes involved in the detection of microbes and in host immune response such as *NOD2, IL23R,* and *ATG16L1* have been reported by several groups as susceptibility genes for IBD[18-24, 58,59, 72,73,78].

1.1.3. Altered gut microbiome

The human gut microbiome is a vast and tremendously complex system, with an estimated 10^{14} bacterial cells of approximately 1000 species residing in our gut[25]. This bacterial community, in healthy individuals, functions in a symbiotic manner with the host. However, in patients with IBD, there is a shift in the composition of the microbial community[25, 26]. A study by Gevers and colleagues in 2014 illustrated that samples from multiple gastrointestinal locations from early onset CD patients had increased numbers of Enterobacteriaceae*,* Pasteurellacaea*,* Veillonellaceae, and Fusobacteriaceae, while exhibiting a decreased numbers of Bacteroidetes, and Clostridia. Such changes are attributed to alterations in the overall gut environment, in particular the nutrient and oxygen environment which facilitates the growth of facultative anaerobes.

Following inflammation of the GI tract, increase expression of pro-inflammatory cytokines such as interferon-γ (INF-γ) promote the production nitric oxide, ultimately leading to nitrate production on the luminal surface of the gut. Members of the Enterobacteriaceae family have well conserved nitrate reductase enzymes that are able to utilize nitrate for respiration, while other families of obligate anaerobic bacteria such as Bacteroidetes and Clostridia fail to obtain such genes[74-76]. Additional nutrient production from host cells after inflammation promotes the selection of bacteria that can 'bloom' in such environmental niches. Phospholipids on the epithelial surface can be metabolized by microbes to ethanolamine (EA) to become a source of energy for ethanolamine degrading bacteria such as *Salmonella*, *Escherichia coli* and *Clostridium difficile* (*C. difficile*). Increased mucus production on the epithelial surface production is also associated with an inflamed gut. While the mucosal layer is traditionally known for providing a protective barrier for the host against bacterial threat, they are rich in amino acids such as proline, serine and threonine which can be glycosylated and used as a sugar nutrient source for invading microbes. As a result, there is often an enrichment of mucus degrading bacteria associated with inflammation of the GI tract[74-76]. This allows for a yet another nutrient advantage of invading pathogens over commensal bacteria, further narrowing the overall diversity of the gut microbiota. The host inflammatory response is also coupled with several antimicrobial effector mechanisms intended to eliminate infectious pathogens. Epithelial and Paneth cells increase the expression of several antimicrobial peptides in response to colitis. Invading pathogens have formed elegant systems to avoid killing through these peptides, ranging from cell-membrane modifications to expression of proteases that can degrade the peptides[76-77].

Combating these bacteria with antibiotics as a first-line therapy for treating IBD may not be the best practice. Data from Gevers and colleagues' investigation revealed that the microbial community altered significantly more when antibiotics are administered[27]. Additionally, a more recent paper further discussed the link between antibiotics and dysbiosis of the gut. Perturbation of the gut microbiome via antibiotics or diets high in fat and sugar result in a lower production of short-chain fatty acids (SCFA), which are critical in mediating anti-inflammatory responses[60]. This line of reasoning is consistent with hypothesis of colonization resistance which will be discussed below, where loss of protective and beneficial microbes allows the chance for originating the proliferation of other non-beneficial taxa[6,27].

1.2. *Escherichia coli*

1.2.1. *Escherichia coli* as a commensal

Escherichia coli (*E. coli*) is a rod-shaped, gram-negative facultative anaerobe that belongs to the larger family of Enterobacteriaceae and colonizes the colon of the mammalian gastrointestinal tract[1,2]. As a gram-negative bacterium, *E. coli* has two membranes; an inner phospholipid membrane and outer membrane rich with proteins, lipopolysaccharide (LPS), and phospholipids[3]. *E. coli* colonizes the mucosal membrane of the large intestine and is part of our large microbiota population that contains trillions of bacteria functioning in a symbiotic relationship with the host[4,6,44]. *E. coli* is among the first colonizers of the infant GI tract and an individual may be colonized by 10 or more individual strains of this bacterium at any one time. This mucosal colonization occurs as a result of a mixed-species biofilm formation upon the thin layer of mucus coating epithelial cells. The human gut is also protected by immunoglobulin A (sIgA), an antibody important in both the prevention of bacterial overgrowth and subsequent translocation, and in facilitating biofilm formation of beneficial gut microbes. In particular, a study conducted by Bollinger and colleagues found that sIgA increased *E. coli* adherence to live cultured epithelial cells by 64%[45]. Once colonization occurs, the nutrient source within this niche environment is from shed epithelial cells, diet-derived nutrients fiber and mucosal polysaccharides. *E. coli* is unable to degrade these polysaccharides; therefore, the species relies on other anaerobic bacteria within the mucosal layer to degrade these polysaccharides into smaller mono- and di-saccharides via secretion of extracellular polysaccharide hydrolases[6].

This relationship between commensal *E. coli* and other anaerobic microbes in the mixed biofilms is referred to as the "Restaurant" hypothesis. In this hypothesis, commensal *E. coli* can associate with their own respective polysaccharide degrading mixed anaerobe species, which are able to 'feed' the degraded sugars to *E. coli.* Different commensal *E. coli* inhabit different 'restaurants' (or mixed species biofilms), ultimately leading to different metabolic capabilities depending largely on the population the commensal resides in[79]. In return, *E. coli*, among other commensal microbes, aid in the production of various nutrients and vitamins for the host, while the host provides an environmental niche enriched with nutrients of its own that allow the microbial communities to thrive within[4,5]. In particular, commensal bacteria directly protect the

host from being colonized with potentially harmful microorganisms through a process of competitive exclusion. This mucosal protection, formally termed colonization resistance, occurs via the microbial community being able to out-compete invading species for limiting nutrients, thus making it difficult for new microorganisms to survive in a dense and competitive population of bacteria. The fundamental basis of this colonization resistance follows Dr. Rolf Freter's nutrient-niche hypothesis, which states that in order to successfully colonize and persist in the intestine, bacteria must grow faster and also be able to use at least one limiting nutrient better than all other bacterial species present in that community[6]. Disruption of this dynamic bacterial ecosystem can lead to invading pathogenic microbes to successfully colonize the intestine and become a source for infectious disease.

1.2.2. Pathovars of *E. coli*

E. coli is one of the best characterized and widely used prokaryotic model organisms. Most studies using *E. coli* as a model organism are completed with non-pathogenic, lap-adapted *E. coli* strains called K12. However, in reality, there is large amount of variation between commensals, lab-adapted strains and pathovars of *E. coli*[80,81]. What makes *E. coli* a commensal is successfully colonizing the colon without producing adverse effects to a healthy host at normal concentrations[82]. On the other hand, well-studied pathovars such as enterohemorrhagic *E. coli* (EHEC), uropathogenic *E. coli* (UPEC) and enteropathogenic *E. coli* (EPEC) differ through the utilization of virulence factors such as adhesion genes and secretion systems acquired through horizontal DNA transfer, ultimately leading to pathogenicity. For instance, in addition to symptoms of severe abdominal pain and diarrhea, a hallmark of both EHEC and EPEC infection is the presence of attaching and effacing (A/E) lesions on the intestinal epithelial surface. This phenotype is attributed to the acquisition of a large pathogenicity island called the locus of enterocyte effacement (LEE) which codes for the adhesin intimin, a type III secretion system (T3SS), various effectors including a translocated intimin receptor (Tir)[82-85]. A/E lesions form in a highly organized manner by responding to environmental ques such as different carbon sources, hormones, and autoinducers[85]. UPEC, the main etiological agent for urinary tract infections (UTI), also has distinct virulence gene expressions that allow it to successfully colonize and replicate within the urinary tract. Snyder and colleagues (2004) analyzed the

transcriptome of UPEC strain CFT073 after CBA/J mouse infection. They found of the 313 upregulated genes, 45 did not have homologs in *E. coli* K12. The majority of these genes encoded for virulence factors associated with iron uptake systems, fimbrial adhesion genes (primarily type 1 fimbriae), and capsular synthesis. Interestingly, the group reported up to a 4-fold increase in the induction of genes coding for microcins, which are small antibiotic compounds often secreted by bacteria to outcompete other bacterial strains, illustrating the competitive edge this UPEC gains in a harsh and nutrient limiting area[86]. These examples highlight the diverse nature of *E. coli* as a bacterium, where it can be identified as a symbiont in the human gut microbiome, or a pathogenic microbe capable of causing severe disease.

1.3. Adherent-invasive *Escherichia coli*

Early work in 1978 showed that *E. coli* antibody titers were higher in both CD and UC patients when compared to a control population[87]. Since then, there has been extensive work to characterize a pathovar of IBD-associated *E. coli.* More recent studies from the Darfeuille group found that *E. coli* was highly prevalent (50-100%) upon analysis of the aerobic and anaerobic bacterial community associated with the ileal lesions of CD patients[28,29]. Isolates from both chronic and early ileal lesions showed enhanced ability to better adhere to Caco-2 cells (84.6% and 78.9% respectively) when compared to isolates from healthy controls (33.3%). One of the CD ileal isolates called LF82 showed that in addition to its adherent property, the strain has been reported to invade and persist within phagocytic cells such as macrophages[29,88-90]. Screens attempting to find virulent genes such as *eae* encoding for intimin in EHEC and EPEC or *ipaC* encoding for an invasin protein in *Shigella flexneri* in the IBD-associated *E. coli* isolates showed that these strains lacked any of the known virulence genes in other enteric pathogens[28]. Therefore, a new pathovar of *E. coli* called adherent-invasive *Escherichia coli* (AIEC), distinguished by its ability to invade epithelial cells, was created[28, 29].

1.3.1. Adhesion

While the adherent and invasive role of this bacteria is well established, the mechanisms by which this occurs is not well-characterized. As stated above, AIEC does not possess known

type III secretion systems or exotoxin virulence genes common to different pathogenic *E. coli* strains such as EPEC, entero- toxigenic *E. coli* (ETEC), or EHEC, leaving numerous unresolved questions about how the bacterium might contribute to IBD pathogenesis. Despite the lack of obvious virulence factors, several groups have examined specific adhesins that might contribute to host colonization.

Common to most *E. coli* species are filamentous appendages called pili. Of these proteins, the most commonly found pili called the type 1 pili is involved in adhesion to various eukaryotic cell surfaces such that are rich in mannosylated glycoproteins. The entire pilus is composed of nine genes that encode for the protein itself, chaperone and usher proteins, and transcriptional regulators of the major subunit *fimA*. FimH is the adhesion located on the tip and is primarily responsible for the binding of mannosylated glycoproteins[89]. In 2001, Boudeau and colleagues showed evidence that AIEC strain LF82 uses a type 1 pili variant to adhere and invade intestinal epithelial cells. To confirm the role of the type 1 pili in the adherence and invasion properties of LF82, the group screened for an identified 11 non-invasive mutants in the strain using transposon mutagenesis within the *fim* operon. Of the 11 mutants, 10 resulted in complete loss of the type 1 pili, while the remaining mutant reduced type 1 pili synthesis. Nine out of the 11 strains, all of which lost the ability to synthesize the type 1 pili, showed reduced ability to adhere to and invade intestinal epithelial cells. Two strains that had insertions in *fimF* and *fimI* did not show changes in adherence of the strain. The *fimF* mutant resulted in the reduced type 1 pili synthesis, while the function of *fimI* is not well understood. When these non-invasive *fim* mutants were complemented with the entire type 1 pili operon, invasion phenotypes were restored to wildtype LF82 levels. Interesting, the complementation of the entire type 1 pili operon from LF82 to a non-invasive *E. coli* strain did not result in an 'invasive switch', insinuating strain-specific accessory genes and proteins involved in the overall adherence and invasive phenotype of LF82[89]. Further, in 2007, Barnich *et al.* showed that there was an upregulation of glycosylated receptors of the type 1 pili variant called carcinoembryonic antigen–related cell adhesion molecules 5 and 6 (CEACAMs) on the apical surface of the ileal epithelium from CD patients[31]. The authors illustrated that the type 1 pili from LF82 preferentially binds CEACAM6 to manifest its invasive phenotype, shown by decreased LF82 adhesion after pretreatment of ileal enterocytes from CD patients with anti-CEACAM6

antibodies. In 2009, Carvalho *et al.* expressed CEACAM6 in transgenic mice in order to determine if the AIEC strain LF82 could colonize the intestinal mucosa and induce subsequent inflammation. The authors found that strain LF82 was able to colonize the mucosal layer in the transgenic mice, and produced several pathogenic phenotypes including colitis, rectal bleeding, mucosal inflammation, increased proinflammatory cytokine expression, and weight loss[30]. These findings suggest 1) patients with overexpression of CEACAM6 might be at an increased risk of establishing the onset of IBD, and 2) elevated ileal expression of CEACAM6 might act as a biomarker for CD in undiagnosed patients.

1.3.2. Metabolic adaptability

The gut epithelial surface is highly colonized area where commensals and AIEC pathovars must compete for nutrients and resources. Critical for survival is exploiting different metabolic pathways and nutrient sources to create a metabolic niche in which the bacteria can thrive. AIEC strains have shown several ways to accomplish this. A recent study looking at the transcriptome of LF82 after exposure to bile salts highlighted up regulation of several gene clusters associated with degradation pathways[91]. In response to bile salts, 17 genes in the *eut* operon, which includes genes for the degradation and utilization of ethanolamine, were up-regulated significantly (2.3 to 12.2-fold). When compared to a non-AIEC strain, LF82 grew more efficiently in minimal media supplemented with EA as the sole nitrogen source which correlated with significantly higher expression of genes in the *eut* operon in LF82 vs. non-AIEC strains. To associate this observation with intestinal colonization in mice, the authors orally challenged mice with a 1:1 ratio of LF82 and LF82Δ*eutB*, a mutant unable to use EA as a nitrogen source. LF82 was significantly enriched in stool samples and ileal and colonic tissue when compared to LF82Δ*eutB*, showing an overall increased fitness advantage[91]. The same authors also reported significant up-regulation of genes in the *pdu* operon, a cluster of genes used in the degradation of 1,2-propanediol, the byproduct of fucose fermentation. While 1,2-propanediol utilization systems are present in other gram-negatives such as *Salmonella*, they are not commonly found in non-AIEC *E. coli* strains. This form of fucose and subsequent propanediol utilization not only gives AIEC a unique competitive edge in nutrient sources, but also might enhance invasion and replication in macrophages as is seen in *Salmonella*[91-93]. Another similar approach looking at the entire genome of phylogenetically diverse AIEC isolates

from CD patients, mice with ileitis, and dogs with colitis showed elevated expression of both the *pdu* operon and the *chu* operon, which encodes for iron acquisition genes. Iron was shown to be essential for the growth of AIEC. Nutrient rich broth treated with iron chelator 2,2'-dipyridl significantly decreased growth of AIEC strain CUMT8. The growth decrease was restored through the addition of ferrous at levels higher than the 100μM. Additionally, elevated production of *chuA*, a gene encoding for a heme iron acquisition protein, resulted in enhanced survival inside macrophages[93]. These examples highlight the metabolic adaptability of AIEC as a pathogen, where it can utilize diverse pathways to gain a competitive edge in a nutrient scarce environment.

1.3.3. Animal infection models

Several attempts at establishing an animal model for AIEC infection have been described. In 2009, Carvalho *et. al* introduced using CEABAC10 transgenic mice, which express humans CEACAMs, to test whether LF82 could colonize the intestinal mucosa and cause subsequent inflammation. While LF82 was unable to colonize wild-type mice, the strain successfully colonized and caused severe inflammation in the transgenic mice after being orally challenged. A loss of colonization in this mouse line was shown after using a LF82 non-piliated mutant, confirming the role of the type 1 pili and CEACAM6 receptor interaction for the adhesion of LF82 to the mucosal surface[94]. A critical component of this AIEC infection model was to pretreated mice with a colitogenic chemical called dextran sulphate sodium (DSS) to induce colitis chemically. In 2013, members from the Coombes lab established another AIEC-mouse infection model that did not need coadministration of a chemical or a transgenic mouse line. The group used another AIEC strain NRG857c to infect streptomycin-treated conventional mice. NRG857c was able to outcompete LF82 when both strains were inoculated at 1:1 ratio in CD1 mice and showed consistently higher bacterial load when both strains where monocolonized. Upon NRG857c infection, the authors showed evidence for chronic inflammation within the gut, with pronounced phenotype present in the caecum. Interestingly, while levels of AIEC fell below the threshold for detection in mouse strain C57BL/6, the inflammation phenotype within the gut of the mice persisted. This phenomenon, as noted by the authors, provides insight into the

potential lasting effect left by AIEC on the gut even after the bacteria is cleared or reduced to a miniscule scale[32].

1.4. Host defense peptides

1.4.1. Classes and structure

Host defense peptides (HDPs) are cationic amphiphilic peptides that are present as an integral part of the innate immune system. The general structure of these antimicrobial peptides can be defined as <100 amino acids in length, with an overall positive charge, and containing a large portion of hydrophobic residues[33]. These peptides are found in abundance within mammals as they are expressed by a number of cells, including epithelial cells within the gut. Two primary classes of HDPs present in humans that contribute to intestinal epithelial defense include defensins and cathelicidins. Defensins are separated into two distinct classes, α-defensins and β-defensins, both of which are stabilized through disulphide bounds between six cysteine residues[95-97]. Both defensin classes have similar tertiary structures because of three disulphide bonds that result in triple stranded β-sheet structures with a β-hairpin loop that contains the cationic residue. In α-defensins, the disulphide bonds are between cysteine residues C1-6, C2-4, and C3-5, and in β-defensins, the disulphide bonds are between C1-5, C2-6, and C3-6[96,97]. α-defensins are most prominently found in the granules of granulocytes in mammalian cells, such as the human α-defensins human neutrophil peptide (HNP) 1-4, which are abundant proteins in neutrophils. Other α-defensins called HD-5 and HD-6 are found expressed in the small intestinal crypts and within the granules of Paneth cells[96,97,100]. Conversely, β-defensins are more widely distributed throughout the body and can be sub-characterized in terms of expression. For instance, human beta-defensin-1 (hBD1) is constitutively expressed by intestinal epithelial cells, while hBD2 and hBD3 are up-regulated after enteric pathogen invasion and with inflammatory disorders, respectively[95,97]. LL-37, the only characterized human cathelicidin, is a dynamic HDP that is expressed by neutrophils, monocytes, natural killer (NK) cells, T cell, B cells, and in the GI tract[97]. LL-37 is capable of stimulating a wide range of responses including pro- and anti-inflammatory activities, wound healing, chemoattractant for immune cells, antimicrobial activity

and much more[36,97]. As a first line of defense, both classes of HDPs represent a critical mechanism of host-intestinal defense against microbial threat.

1.4.2. Mechanisms of action

A common site of HDP expression is on the mucosal layer that covers epithelial cells in animals[35]. Initial HDP-mediated protection against bacteria, particularly of interest, gram-negative bacteria such as *E. coli*, relies on the electrostatic bonding of cationic peptides with negatively charged surfaces on bacterial membranes such as LPS. Once initial attraction towards the negatively charged surface is established, the peptide inserts into the bilayer and form transmembrane pores, disrupting the bacterial surface and ultimately leading to leakage of cellular content[33,34,95-97]. In addition to membrane rupture, there is also evidence of peptides having an intracellular mode of killing. After translocation into the cytoplasm, different HDPs can inhibit cell-wall, nucleic-acid, and protein synthesis and/or intracellular enzymatic activity[34]. Regardless of the specific mechanism of action, the net result is to reduce the bacterial load on the colonized mucosal surface, thereby contributing to host defense. The thinning of the mucosal layer after inflammatory flares of patients who suffer from IBD is associated with elevated production and localization of HDPs to the mucosal surface. In 2013, Meish *et al.* showed that there was increased expression of hBD3 in the biopsies from the terminal ileal of patients with CD compared to those from healthy controls[98]. In addition, another group showed that there was increase in LL-37 expression in both inflamed and non-inflamed patients with UC[99]. The host response in elevated production of antimicrobial peptides is critical in maintaining mucosal tolerance of a changing microbial community. However, bacteria with intrinsic HDP resistance could exploit survival in such harsh conditions produced by the host and help manifest the pathology of IBD.

1.4.3. HDP resistance

Bacteria have evolved various mechanisms to evade killing by HDPs. *Staphylococcus aureus* (*S. aureus*), a gram-positive species that is a common source of both nosocomial and community infections, secretes a protein called staphylokinase (SAK) which bind α-defensins to render them inactive[77,100]. Jin and colleagues (2004) tested 19 *S. aureus* strains against the

bactericidal properties of α-defensins HNP1 and HNP2 and found that strains which produce SAK were effectively protected against the bactericidal activity of the peptides[100]. Other common bacterial resistance mechanism involves modifications to the cell membrane to reduce the overall negative charge. Lipid A, the bioactive component of LPS found on the gram-negative bacterial outer membrane contains anionic phosphate moieties. Several groups have shown that pathogens such as *Salmenolla* and *Pseudomonas aeruginosa* modify lipid A through the addition of positively charged aminoarabinose, altering the net membrane charge and enhancing the resistance of these microbes to cationic peptides[77,101-103]. Additional resistance mechanisms in *Salmonella* include using outer membrane proteases to cleave HDPs directly[103]. Guina *et al.* (2000) showed that strains expressing outer membrane protease PgtE had elevated resistance to α-helical peptide C18G through peptide degradation at one of the three putative *pgtE* cleavage sites[104]. Further, several bacterial species use efflux pumps to protect against cationic antimicrobial peptides (CAMPs). *Neisseria gonorrhoeae*, the causative agent of the sexually transmitted disease gonorrhea, uses the MtrCDE efflux pump to actively export antibiotics, dyes, detergents, and HDP LL-37[102]. The examples listed above are some of the many ways bacterial pathogens have evolved to escape killing from HDPs. The variety in resistance strategies highlights the need to better understand how these bacteria respond to antimicrobial threat.

1.5. Two-component systems

1.5.1. Structure and function

Two-component systems (TCSs) are common prokaryotic signaling systems that enable organisms to have an adaptive response to the microenvironments they reside in consists. They typically consist of two major players, a membrane-bound histidine kinase (HK) sensor and the cognate response regulator (RR). The former is traditionally known as the 'input' component of the pathway, where an appropriate stimulus interacts with the extracellular or periplasmic domain of the HK to cause an autophosphorylation reaction on a conserved histidine residue[49,50,51]. Typically, the cytoplasmic core of the HK consists of two distinct domains: the C-terminal catalytic and ATP-binding (CA) domain, and a dimerization and histidine

phosphotransfer (DHp) domain[51]. The initial phosphorylation occurs through an ATP-dependent mechanism where the CA domain binds ATP and carries the catalytic reaction of transferring the phosphryl group from ATP to a conserved histidine residue located on the DHp domain[50,51].

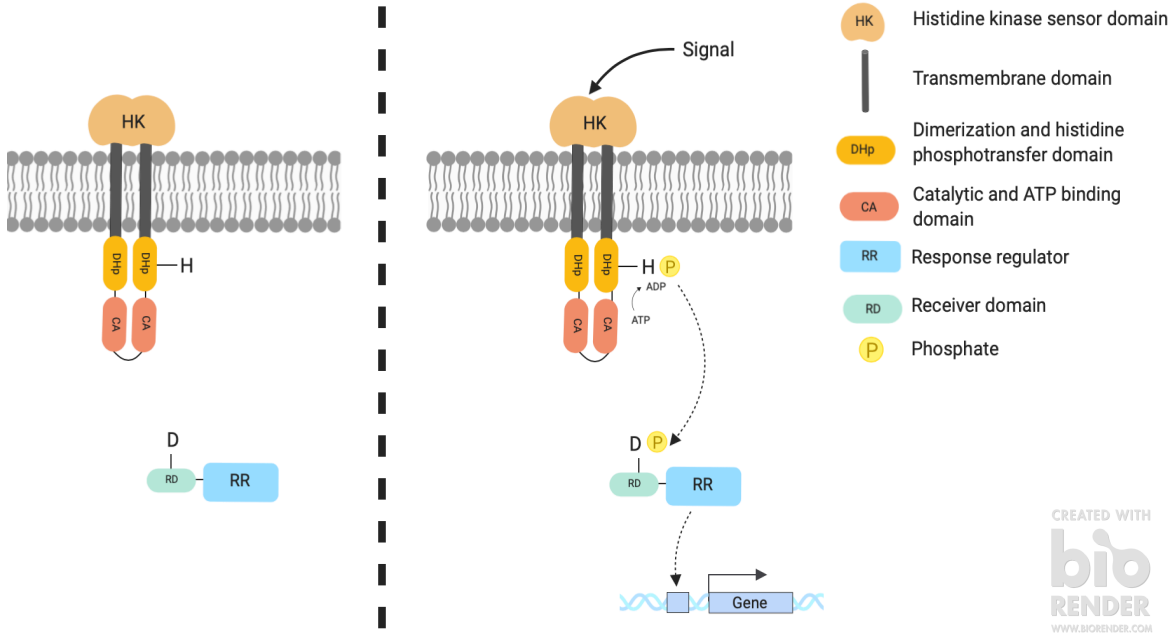

Figure 1. Visual representation of the classical two-component pathway.

Upon inducing stimulus, there is a phosphorylation of the conserved histidine residue on the DHp domain on the histidine kinase. Subsequently, there is a phosphor-transfer to the receiver domain on the response regulator, which activate the protein to regulate genes downstream.

Upon HK autophosphorylation at the histidine residue, two separate modes of action can occur to propagate the signal downstream to the RR, either a classical two-component pathway, or an unorthodox phosphorelay pathway depending on the structure of each respective system. In the classical pathway, upon autophosphorylation of the conserved histidine residue, there is a transfer of the phosphoryl group to the aspartate residue located on the receiver domain of the RR (**Fig. 1**)[1]. The latter phosphorelay pathway involves a hybrid HK which has a receiver domain of its own. It has been estimated that roughly 25% of HK have this additional receiver domain, suggesting that this 'unorthodox' pathway is actually rather common among TCS signaling pathways[1,51]. In this pathway, after autophosphorylation the phosphoryl group is

transferred from phosphor-his to the receiver domain located on the C-terminus of the HK. Following this, a histidine phosphotransferase (HPt) domain receives the phosphoryl group from the HK receiver domain and shuttles the phosphoryl group to the receiver domain found on the cognate RR (**Fig. 2**)[1]. For TCSs, these HPt domains do not possess any kinase or phosphatase activity, therefore it is proposed to be involved as means of extra-regulatory measures[51].

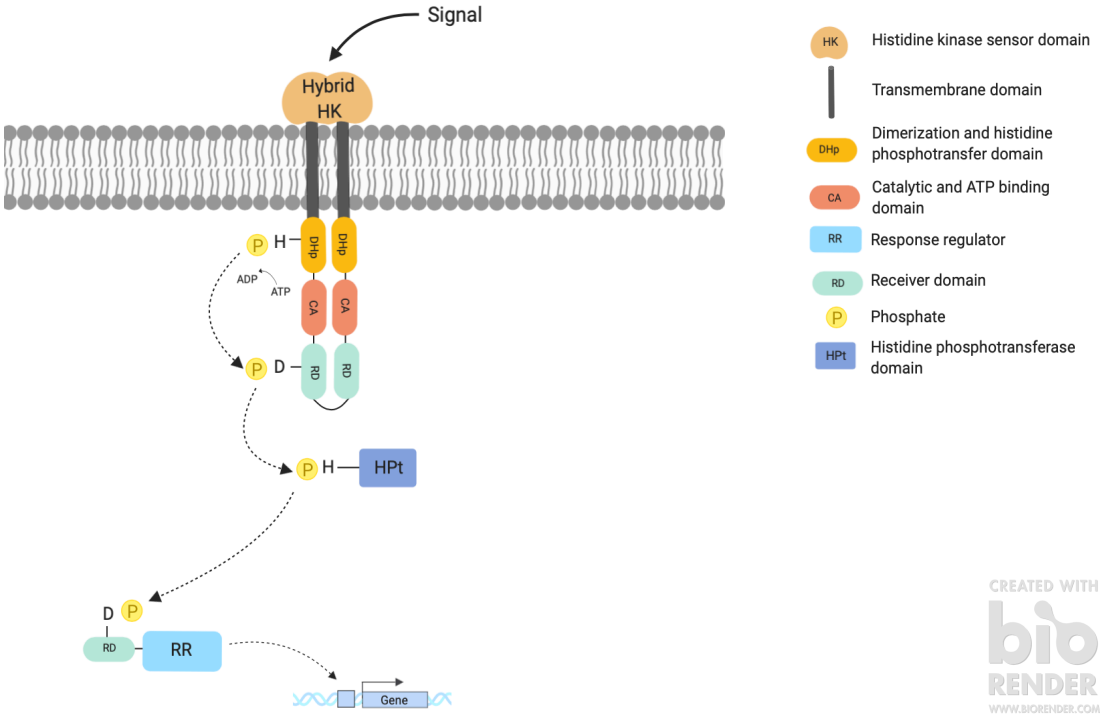

Figure 2. Visual representation of the unorthodox two-component pathway.

Upon inducing stimulus, the histidine kinase phosphorylates the histidine residue on the DHp domain, and subsequently transfers the phosphate to its own REC domain. The histidine phosphotransferase shuttles the phosphate to the REC domain on the response regulator, which activate the protein to regulate genes downstream.

The terminal RR is responsible for the 'output' response produced by a TCS, often leading to alterations in gene expression. Prototypical RR consist of two domains, an N-terminal receiver (REC) domain, and an effector domain[51]. The REC domain is approximately 120 residues which is bond with α/β folds and is found is two states, either active or inactive. The switch between the active or inactive state depends on phosphorylation from the HK. Upon

phosphoryl transfer from the HK to the REC domain of the cognate RR, there is a conformational change in the RR that renders the REC domain active[1,50,51]. The phosphorylation of this domain occurs at a conserved aspartate residue found on the loop that is after β3 fold[51]. Following this, the active REC domain is able to modulate the effector domain, which elicits the output response often through regulating transcription via DNA binding. For instance, in the well-studied PhoPQ TCS, the RR PhoP binds a repeat of a two 7bp binding motifs spaced by a 4bp insert in-between them. This binding motif is called the *pho* box and is found on the promoters of many PhoP regulated genes[52]. Therefore, when the PhoP RR is phosphorylated, it directly binds, with high affinity, to the binding motif of the several downstream genes as a dimer to induce gene expression.

Despite the name, many HK have phosphatase activity their toward respective cognate RR's as well. When stimulating conditions are lost, the HK is able to effectively dephosphorylate the RR to rapidly stop the signaling pathway. A well-characterized example of this is within the EnvZ-OmpR TCS. This system, which is responsible for regulating responses to changing osmolarity, has a HK sensor (EnvZ) that is capable of autophosphorylation, phospho-transfer to its cognate RR OmpR, and subsequent dephosphorylation of phospho-OmpR (OmpR-P)[53]. As such, the output generated by such TCSs is generally controlled through the status of these bifunctional HK. Such bifunctionality is proposed to be used to avoid crosstalk by different TCSs. Down regulation of a cognate RR via phosphatase activity assures that there is no unintended phosphorylation from another a non-cognate HK and also allows rapid responses to changing environmental conditions. In addition, this allows for the suppression of non-cognate RR phosphorylation through constant phosphatase activity during unstimulated conditions, allowing for a more regulated mechanism of inducing each respective TCS[54]. One of the proposed phosphatase activities from HK is thought to occur on the DHp domain, with the conserved histidine residue playing an important role. One of the possible dephosphorylation mechanisms is through reversal of RR-phosphorylation to the His residue on the HK[50,51]. Conversely, several other dephosphorylation mechanisms must exist, as HK mutants that lack the histidine residue still possess phosphatase activity, insinuating another mode of action (**Fig. 3**)[50,51].

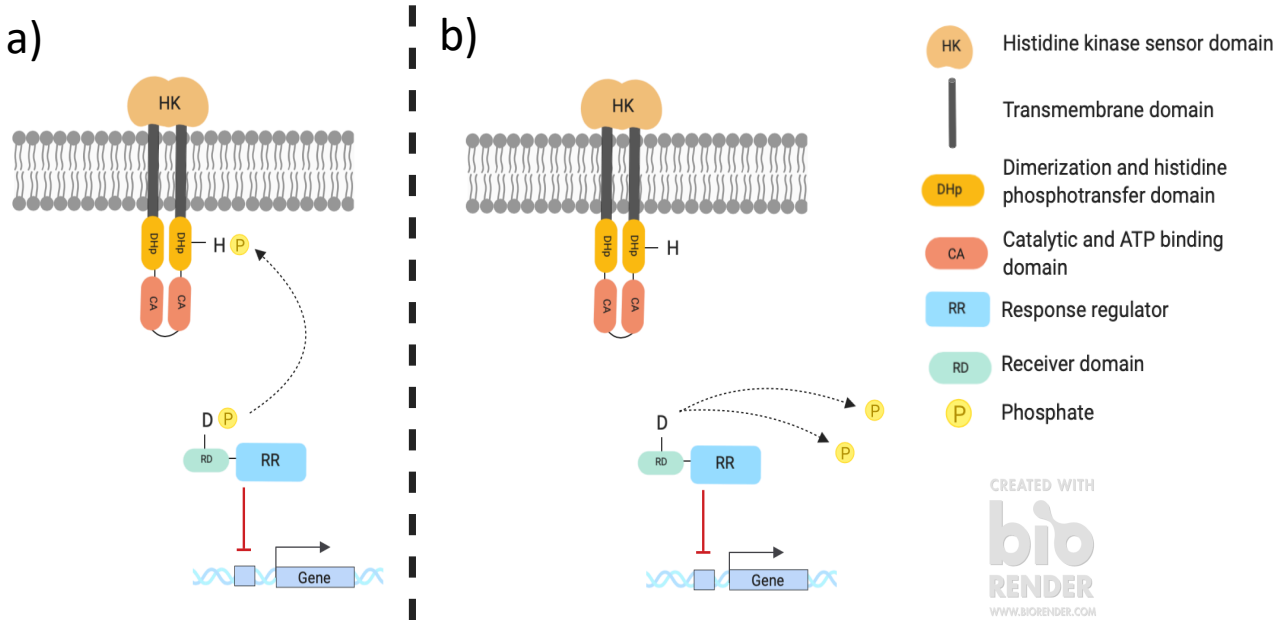

Figure 3. Phosphatase activity from the histidine kinase sensor.

a) reverse phospho-transfer to the conserved histidine residue on the histidine kinase. b) reverse phospho-transfer independent method leading to dephosphorylation of the aspartate residue on response regulator.

Accessory proteins can play a role in the dephosphorylation of the RR. An example of such an interaction is a small 47 amino acid protein called MgrB with the PhoQ HK sensor. Upon sensing of antimicrobial peptides or low magnesium conditions by PhoQ HK sensor, there is an increase in PhoP phosphorylation, which leads to subsequent increase of PhoP regulated genes. This upregulation includes an increase in the transcription of *mgrB*. Goulian and colleagues (2009) demonstrated that after translation, MgrB localized to the inner membrane, orientating in a way where the N-terminus is exposed to the cytoplasm and the C-terminus is facing outwards towards the periplasm. To verify MgrB and PhoQ interaction, they performed a bacterial two-hybrid assay which showed for evidence of a physical interaction between MgrB and PhoQ. Deletion of *mgrB* resulted in a dramatic increase in transcription of PhoP regulated genes, and conversely, over expression resulted in significantly lower transcription of PhoP regulated genes in both inducing and non-inducing conditions[55], thus suggesting that MgrB plays a role in the regulation of PhoQ activity.

1.5.2. PhoPQ-PmrD-PmrAB signaling system

Of interest to the McPhee lab are the PhoPQ and PmrAB TCSs. As briefly discussed above, within the PhoPQ TCS, PhoQ is the histidine sensor kinase that is involved in the detection of cationic peptides and is also induced in limiting conditions of divalent cations such as Mg^{2+}. The PhoQ sensor has two transmembrane regions, a periplasmic sensor domain, and a cytosolic domain that is responsible for the catalytic output. Bader *et al.* (2005) examined the crystal structure of the *Salmonella* PhoQ sensor domain and demonstrated that there is an acidic surface on the sensor domain that closely interacts with the inner membrane. This acidic surface is negatively charged and requires divalent cations to form cationic bridges as means to interact with the negatively charged inner membrane. Divalent cations such as Mg^{2+} bind pockets within the acidic region of the periplasmic sensor domain, rendering PhoQ inactive, where it represses autophosphorylation of its own cytosolic catalytic domain. Antimicrobial peptides such as HDP LL-37 are small, positively charged molecules, and they therefore target the negatively charged head groups of phospholipids within the membrane. As such, these antimicrobial peptides come into close contact with the divalent cationic bridges resulting in competition for the negatively charged binding pocket on the acidic surface. This leads to the divalent cations being displaced, causing a conformation change that allows the autophosphorylation event on the catalytic domain to take place[55,56]. After activation, PhoQ phosphorylates the response regulator PhoP, which induces the expression of several genes downstream[39]. Two genes under the regulation of the PhoPQ TCS are *pagP* and *pmrD*. The PagP enzyme is involved in the transfer of palmitoyl groups from glycerophospholipids (GPL) to lipid A, the bioactive component of LPS that is recognized by the TLR4/MD2/CD14 innate immune receptor complex. This palmitoyl transfer increases the hydrophobicity of the outer membrane, which protects from HDPs[39,40]. PmrD is a protein downstream of the PhoPQ TCS which serves as a connector protein to another TCS called PmrAB (**Fig. 4**)[39, 41,43]. In this TCS, PmrB is the sensor kinase, and PmrA as the RR. PmrAB responds to a variety of stimuli such as high Fe^{3+}, low pH and bile salts[115]. After induction with such stimuli, PmrB phosphorylates PmrA, resulting in activation of several genes downstream. PmrB is also a bifunctional HK sensor, in that this protein has the ability to dephosphorylate PmrA to stop the signaling pathway. The PhoP regulated PmrD protein physically blocks phospho-PmrA from being dephosphorylated by PmrB, ultimately leading to

robust activation of downstream genes that are involved in lipid A modification[41]. The net effect of this activation is addition of aminoarabinose to lipid A results in a lower overall negative charge on the LPS structure, allowing the bacteria to avoid killing via HDPs[42,43].

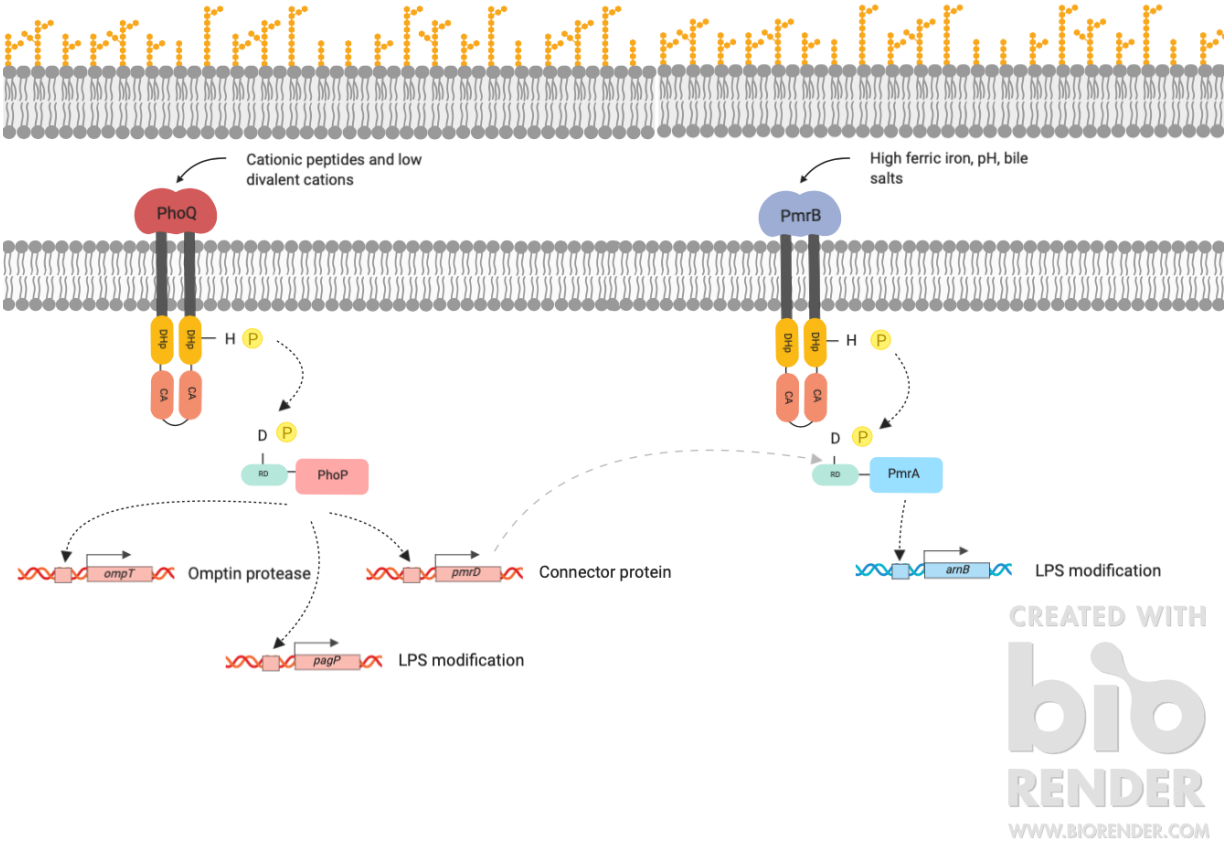

Figure 4. Schematic of the PhoPQ-PmrD-PmrAB two component system in *E. coli*.

As discussed above, HDPs commonly target the negative charge on bacterial membranes. As a result, bacteria have evolved intricate systems to avoid this peptide-mediated method of killing. These systems include either modifying the targets of HDPs, such as LPS on gram-negative outer membranes, or secreting outer membrane proteases involved in the degradation of HDPs (Unpublished data; Aziz, Cho and McPhee). In support of this, McPhee and colleagues illustrated in 2014 that AIEC strain NRG857c resist killing by HDPs through genes located on the plasmid-encoded genomic island (PI-6). Important to this effect are two proteins, *arlA* and *arlC*, encoding a Mig-14 family protein and an OmpT family outer membrane protease that is capable of cleaving LL-37, respectively[47]. While the role Mig-14 in resistance to HDPs is not yet

well understood, the role of *ompT* in degrading α-helical peptides is established, as was illustrated by Thomassin *et al.* in 2012[48]. These resistance outputs are under the regulation of a network of bacterial-sensing systems called two-component systems. In accordance to this, bacteria that display a broad range of metabolic diversity encode more TCSs in their genome than other bacteria that inhabit more of a uniform environment[37].

2. Hypothesis and Objectives

2.1. Rationale

Given the up-regulation of HDPs by the host and an increased presence of AIEC in patients with IBD, earlier work in the McPhee lab completed by graduate students Youn Hee Cho and Michael Renouf looked at resistance phenotypes of clinical strains of these IBD-associated *E. coli* (from now on, referred to as IBDEC) to HDPs LL-37 and hBD-3. Strains displayed a wide variety of resistance phenotypes, varying between completely susceptible to highly resistant for both LL-37 and hBD3 peptides (**Fig. 5**). In general, hBD-3 resistance is enriched in CD isolates, while LL-37 resistance is enriched in UC isolates. This variable phenotypic output forms the fundamental rationale behind my project: what is the underlying mechanism behind the heterogeneity in these resistance phenotypes among different strain of IBDEC?

The PhoPQ and PmrAB TCSs represent a mechanism by which IBDEC can respond and elicit resistance to HDPs. While a lot of previous work has been completed looking at TCS response to different concentrations of stimuli, insight into how genetically similar strains differentially responding to the same signal has yet to be determined. Most work in a laboratory setting using *E. coli* as a model organism is completed using K12 lab strains. These strains are experimentally evolved and well adapted to various growth and stressed conditions. As a result, they often yielding a consistent phenotypic output. Using non-lab adapted clinical strains allows for differentiation of a genetically similar bacterial groups into subpopulations with distinct phenotypes. Such distinct phenotypic outputs could provide insight as to how these different strains sense and respond to a fluctuating environment. Therefore, as a means to investigate the observed variation in HDP resistance, we hypothesize that the clinical isolates of IBDEC are able to differentially respond to the same stimulus of both the PhoPQ and PmrAB TCSs and that this difference may lead to elevated HDP resistance in those strains.

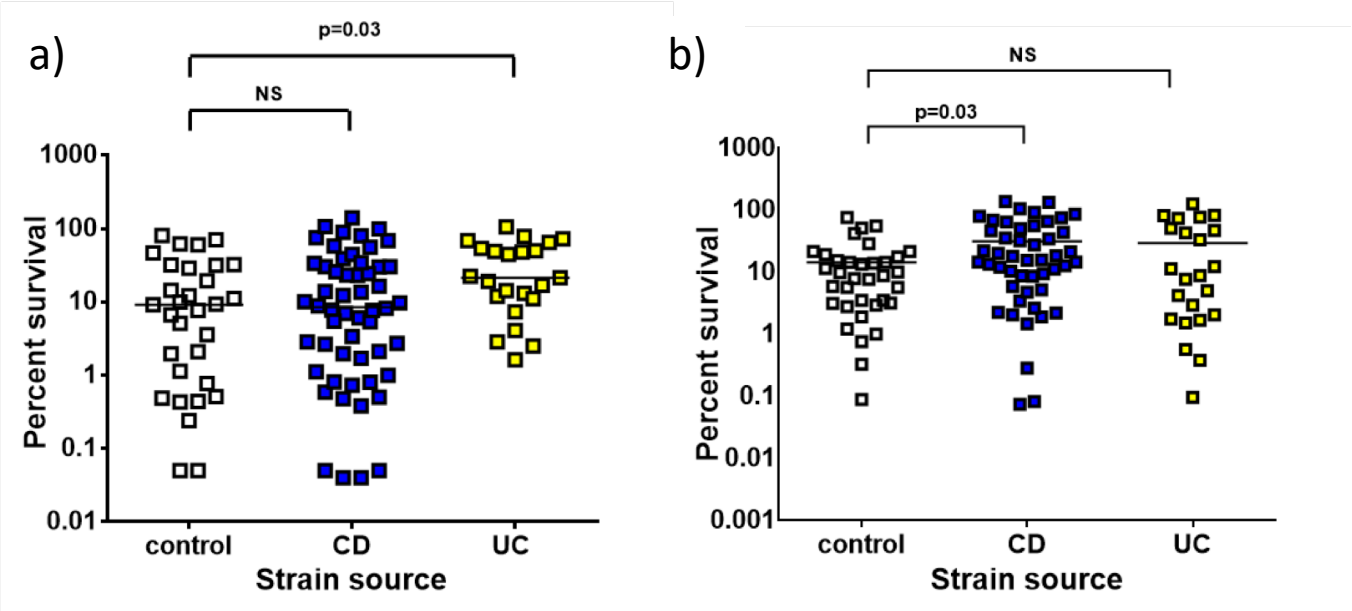

Figure 5. Resistance to LL-37 (a) or hBD3 (b) in IBDEC varies by the disease state of the patient from whom the strain was isolated.

2.2. Hypothesis

There is heterogeneity among IBDEC strains in the induction level of the PhoPQ and PmrAB TCS regulated genes using the same concentration of inducing stimulus and this heterogeneity contributes to HDP resistance.

2.2.1. Objective I

Fuse promoter regions of representative genes downstream of each TCS with a green fluorescent protein. Clone fusions into plasmid to serve as a toolbox for subsequent fluorescence assays. The promoter regions selected are *arn* operon, *ompT* and *pmrD*.

2.2.2. Objective II

Transform the constructs into a panel of clinical CD isolates for analysis of TCSs induction under stimulating conditions. The output will be measured using a fluorescence assay,

measuring *arnB, ompT* and *pmrD* promoter activity. Here we will examine two distinct outputs of gene expression, absolute level of expression (measured in RFU/OD600) and fold-induction in response to a set of standardized inducing conditions.

2.2.3. Objective III

Measure polymyxin B resistance in IBDEC strains under varied Mg^{2+} concentrations to correlate any observed heterogeneity in Mg^{2+} dependent gene expression with a phenotypic output.

2.2.4. Objective IV

Perform western blots for HA-tagged PhoP in the panel of CD isolates and K12. Following this, levels of PhoP phosphorylation for each strain will be determined by using phos-tag gels.

3. Methods

3.1. Amplification of *arnB, ompT* and *pmrD* promoters using polymerase chain reaction

Using a BIO-RAD C1000 Touch™ Thermal Cycler, a polymerase chain reaction (PCR) was performed to amplify the upstream promoter regions of the *arnB*, *pagP* and *pmrD* genes using genomic DNA (gDNA) extracted from a K12 strain of *E. coli* BW25113. Primers were designed (**Table. 1**) and ordered from Sigma Aldrich® in dry form at 100µM stock for the forward (containing the XhoI restriction site) and reverse (containing the BamHI restriction site) strands in order to amplify the promoter region of each respective gene. Primers were resuspended in sterile milli-Q water (MQ-H_20) to make 10X working stocks. A volume of 20µL PCR was prepared for each respective gene. The 20µL reaction contained the following: 10.2µL sterile MQ-H_2O, 4µL High-Fidelity (HF) buffer, 0.4µL 10mM dNTPs, 0.25µL of Phusion® Hot Start II High-Fidelity DNA Polymerase, 4µL primer pair, and 0.5µL BW25113 gDNA. The reaction assembly was performed on ice. As a result, PCR tubes were also prechilled on ice to ensure that an optimal temperature was maintained throughout the process. As a general note, a master mix containing MQ-H_2O, HF-Buffer, dNTPs and Phusion® polymerase was made in a 1.5mL microcentrifuge tube in that order. Subsequently, the master mix was aliquoted into an appropriate number prechilled PCR tubes. Once the master mix was evenly distributed, the primer pair for each respective gene and the gDNA was added. The PCR tubes were centrifuged for approximately 30 seconds before being placed in the thermocycler. The thermocycler was configured to an annealing temperature of 64°C, extension temperature of 72°C, and was run for 30 cycles (**Table. 2**).

Table 1. Primers designed for amplification of *arnB*, *pagP* and *pmrD* promoters from BW25113.

PRIMER	**SEQUENCE**
ArnB-Forward	CTCGAGGTAAACTCCACCTATAGACAAG
ArnB-Reverse	GGATCCTGCTTTTCCTTCCGCCATTG
PagP-Forward	CTCGAGCCCAATAAATTGGCGATG

PagP-Reverse	GGATCCTTGTGACCATAAAACATTTATCAAAAATC
PmrD-Forward	CTCGAGTCAGGCGCTAAAAGAGTGG
PmrD-Reverse	GGATCCTGCATTATCCTGTTTGCTAAG

*****Underlined sequence refers to restriction sites

Table 2. Thermocycler configuration for amplification of *arnB*, *pagP* and *pmrD* promoters from BW25113.

STEP	**TEMPERATURE °C**	**TIME (in seconds)**
Initial	96	60
Denaturing	96	20
Annealing	64	30
Extension	72	30
Final Extension	72	300
Infinite Hold	4	∞

3.2. PCR validation using gel electrophoresis

PCR products were verified using gel electrophoresis. In order to do this, a 1% agarose small gel (6-8 wells) was created using 0.2g of agarose powder, 20mL of TAE buffer and 0.5μL of ethidium bromide. The agarose and TAE buffer was combined into a flask, after which the solution was microwaved to completely dissolve the agarose. Ethidium bromide was added once the solution was cooled to approximately 50-60°C, or enough to be hand-held. Following this, the mixture was quickly transferred to a cast, and combs were placed inside before the mixture began to solidify. After solidification, the gel was submerged in TAE buffer inside the GE-100 MiniRun Gel Electrophoresis System. DNA ladder, either 1 kilobase (KB) or 100 base pair (BP) was added to the first lane for size references. Subsequent lanes were filled with 5μL of PCR product mixed with 0.5μL of Fast Digest (FD) Green Buffer. The gel was run at 100V for approximately 15-18 mins. Following this, the gel was visualized with ultraviolet (UV) light using a Bio-Rad Gel Doc TM EZ Imager machine.

3.3. Amplification of *pagP* and *pmrD* promoters using a temperature gradient PCR

Based on the agarose gel results, successful amplification of the *arnB* promoter was completed based on the size of the band. The band for the *pagP* promoter was absent, therefore this amplification was not successful. It was suspected that the PCR product representing the *pmrD* promoter might be a hybridization of the forward and reverse primers due to the low brightness and molecular size. Therefore, in order to optimize the PCR for *pagP* and *pmrD*, a temperature gradient reaction was performed. This PCR protocol is identical to the one discussed above, with two differences: 1) a 50µL reaction size was used this time, which included: 32µL of MQ-H_2O, 10µL HF buffer, 2µL dNTPs, 1µL Phusion® polymerase, 4µL primer pair and 1µL BW25113 gDNA, and 2) a panel of eight annealing temperatures were used for each respective promoter amplification. The temperature ranged from 60°-70°C. This temperature gradient efficiently determines the optimal annealing temperature for each PCR. Following the gradient PCR, validation through gel electrophoresis was completed as described above.

3.4. PCR product purification

Amplified DNA from the PCR described above were purified using a Geneaid® Presto Gel/PCR DNA Fragments Kit. This high efficiency purification process removes any contaminants, enzymes, salts and unincorporated nucleotides, allowing up to 95% purification of a PCR product. Subsequently, the concentration of the eluted DNA was quantified using a Nanodrop® 2000 Spectrophotometer.

3.5. Cloning purified *arnB, pagP* and *pmrD* promoters into pCR2.1 TOPO Vector

The nature of using high-fidelity polymerases such as Phusion® yields blunt-ends on the DNA being amplified. As a result, prior to inserting these vectors into pCR2.1 TOPO, purified DNA fragments were T-tailed to allow for effective ligation of the promoter inserts into the vector. Purified *arnB, pagP and pmrD* promoters, 5µL of 10X Taq buffer, 1µL of dNTPs, and 0.5µL of Taq polymerase were added to a 1.5mL microcentrifuge tube. After all components had

been combined, the mixture was centrifuged shortly prior to being incubated at 72°C for 10 minutes. Following incubation, the T-tailed DNA fragments were purified yet again, using the same protocol as described above. Once purified, the DNA fragments were cloned into pCR2.1 TOPO. In order to do this, 2μL of each respective T-tailed DNA fragments were combined with 0.5μL of NaCl solution and 0.5μL of pCR2.1 TOPO vector and centrifuged for a short time to ensure contents were mixed. The mixture was incubated at room temperature for approximately 15-20 minutes.

3.6. Transformation of pCR2.1 TOPO with *arnB, pagP* and *pmrD* promoter inserts into MACH1 cells

Chemically competent and fast growing MACH1 cells were used for initial transformations. To do so, MACH1 cells were thawed on ice for five minutes. After being thawed, each respective 3μL pCR2.1 TOPO reactions were added to MACH1 cells. The MACH1 cells + pCR2.1 TOPO went through a process of heat shock, where each tube containing the mixture was placed in a heating block set to 42°C for 30 seconds. Following this, all mixtures were placed on ice to recover for 5 minutes. 500μL of Super Optimal Broth (S.O.C) media was added to each tube, after which all tubes were placed in a shaking 37°C incubator for approximately two hours.

3.7. X-gal screening of transformed MACH1 colonies

The pCR2.1TOPO vector contains a *lacZ*α gene which encodes an enzyme called β-galactosidase that is capable of breaking the glyosidic bond of a sugar. Internally, the *lacZ*α gene has multiple cloning sites (MCS) that can be cut by restriction enzymes to insert fragments of DNA into. Therefore, if DNA is successfully inserted into the vector, the β-galactosidase enzyme will not be expressed. This reporter system can be utilized by using a substance called X-gal. X-gal is a clear liquid compound that contains galactose sugar linked to an indole molecule. β-galactosidase hydrolyzes the galactose in X-gal which yields a bright blue color bacterial colonies. A non-functional called β-galactosidase enzyme cannot breakdown the galactose,

therefore will produce white bacterial colonies. Further, pCR2.1 TOPO also has kanamycin resistance as another mode of selection.

During two hours of recovery described above, lysogeny broth (LB) agar + kanamycin (50μg/mL) plates were prewarmed in a 37°C incubator. After the recovery period was completed, LB + kanamycin plates were prepped for plating of the transformed MACH1 cells. First, each plate was treated with 25μL of X-gal. The X-gal solution was spread evenly using sterilized spreading beads. Once the X-gal solution had dried, each pCR2.1 TOPO transformed MACH1 strains were plated at two volumes, 50μL and 150μL. Once the plates had dried, beads were removed, and all plates were incubated overnight at 37°C.

3.8. Confirmation of pCR2.1 TOPO with *arnB, pagP* and *pmrD* promoter inserts into MACH1 cells

Following overnight incubation, plates were examined for blue and white colonies. 2-3 white colonies were picked and cultured overnight in 3mL in LB + 3μL of kanamycin. The following day, plasmids from overnight cultures were extracted using a Geneaid® High-Speed Plasmid Kit. After successful extraction, plasmids were double digested with an EcoRI restriction enzyme. This digestion separated the promoter inserts from the vector backbone. The digestion reaction included 5.5μL of MQ-H_2O, 0.5μL EcoRI, 1μL FD buffer, and 3μL of vector. The reaction was incubated at 37°C for 10 minutes. Once digestion was completed, a 1% agarose gel electrophoresis was performed. In addition, vectors containing the inserts were sent to an external sequencing facility for Sanger sequencing for verification.

3.9. Subcloning into pCS26

Upon sequence verification, the *arnB, pagP* and *pmrD* promoter inserts were subcloned from the pCR2.1 TOPO vector into a pCS26 plasmid. This plasmid contains a *luxCDABE* reporter system, which encodes for luciferase, an enzyme capable of producing luminescence. The pCS26 plasmid was extracted from using a Geneaid® Midi Plasmid Kit. In order to achieve the subcloning, another digestion reaction was performed using the XhoI and BamHI restriction

enzymes. Purification of the digested vector was performed using the same PCR purification kit mentioned above, however, a gel extraction was completed instead of a PCR product purification. To do this, up to 300mg of the insert bands were excised from the 1% agarose gel under blue light to prevent DNA damage from UV light. The pCS26 plasmid was also digested with XhoI and BamHI and incubated at 37°C for 10 minutes. The digested plasmid and gel purified inserts were ligated together using the following reaction: 2µL of T4 ligase buffer, 2µL T4 DNA ligase, 2µL of double digested pCS26 plasmid, 10µL of gel purified respective promoter inserts and 4µL of MQ-H_2O. The 20µL ligation reactions were incubated at room temperature for 1 hour. After the incubation period, all ligated plasmids were transformed in a DH5α strain of *E. coli* using the same heat shock transformation protocol described above. After recovery, all strains were plated at two volumes of 50µL or 200µL on LB + kanamycin plates, as pCS26 also has kanamycin resistance.

3.10. Verification of *arnB, pagP* and *pmrD* promoters cloned into pCS26 plasmid using colony PCR

Plates were examined for bacterial colonies the following day. Once there was visual confirmation of bacterial growth, colony PCR for each strain was performed to verify the promoter inserts. Colony PCR is an effective screening method to determine if the bacteria colonies have the plasmids of interest with the desired inserts. Plasmid specific primers are needed for colony PCR, therefore, in this case, forward and reverse primers for pCS26 were used. Eight colonies were picked from each plate; therefore, a total 16 total colonies were picked from each individual strain. The colonies picked were used as a source of gDNA for the PCR. The reactions were 20µL and contained the following: 15.75µL MQ-H_2O, 2µL 10X Taq buffer, 1µL dNTPs, 1µL pCS26 primer pair, 0.25µL Taq polymerase. The thermocycler was configured to an annealing temperature of 62°C (**Table. 3**). Following completion of PCR, the products were visualized through a 1% agarose gel described above.

Table 3. Thermocycler configuration for colony PCR.

STEP	TEMPERATURE°C	TIME (in seconds)
Initial	94	180
Denaturing	94	30
Annealing	62	20
Extension	72	60
Final Extension	72	600
Infinite Hold	4	∞

3.11. Luciferase assay monitoring *pagP* and *pmrD* upregulation in BW25113 and Δ*phoP* BW25113

Following colony PCR verification of *arnB, pagP* and *pmrD* promoter inserts into pCS26, all plasmids were transformed into a collection of three *E. coli* strains: BW25113, Δ*phoP* BW25113 and Δ*pmrA* BW25113 using the heat shock protocol described above. After successful transformations, freezer stocks of each strain were created. Luciferase based luminescence assays were performed using black-well, clear bottom 96 well plates. A total volume of 225µL was added to each well. Control wells included either 225µL of N-minimal media with low Mg^{2+}, N-Minimal media with high Mg^{2+}, or LB. Overnight cultures of pCS26-*pagP* in BW25113 and Δ*phoP* BW25113, and pCS26-*pmrD* in BW25113 and Δ*phoP* BW25113 were prepared using 3mL of LB + 3µL of kanamycin. A 1:50 dilution of each overnight culture was used for the experiment. Three biological replicates of each combination of media and strain were arranged. Perimeter facing wells were filled with 250µL of dH_2O to reduce the effect of evaporation during the experiment. After preparing the 96 well plates, a Biotek Synergy HTX Multi-Mode Reader was used to measure luminescence and bacterial growth. The *luxCDABE* bioreporter does not require any substrate or excitation to produce light, therefore the excitation wavelength was blocked, and emission filter was held at the 'hole' position. Luminescence and OD_{600} readings were measured every 15 mins for 12 hours under continuous shaking conditions at 37°C.

3.12. Production of *arnB, pagP* and *pmrD* promoter + green fluorescent protein fusions

In addition to utilizing luciferase activity as a measure for *arnB, pagP* and *pmrD* promoter regulation under inducing conditions using the pCS26 plasmid, *arnB, pagP* and *pmrD* fusions with green fluorescent protein (GFP) were also constructed. GFPmut3, a more unstable version of GFP was used in order to more accurately track changes in gene expression levels. The protocol for creating these fusions involved a three step PCR, termed Single Overlap Extension PCR (SOE-PCR). Primers were generated for the promoter regions of *arnB, pagP* and *pmrD*. In addition, primers were also generated for GFP extracted from a p3174 plasmid. The primers were designed in a way where the end of the reverse primers for each respective promoter had the first 17 nucleotide sequences of GFP. Equally, the start of the forward primer designed for GFP contained approximately the last 20 nucleotides of each respective promoter region (**Table. 4**). Two separate PCRs were completed, one for each promoter region, and one for each promoter specific GFP region. This design enabled overhangs on each PCR product that allows the two products (promoter region and promoter specific GFP) to be 'stitched' together in the third PCR using the forward primer for the promoter, and the reverse primer for the promoter specific GFP.

The first two PCR were 50µL reactions and contained the following: 32.5µL MQ-H_2O, 10µL HF buffer, 2µL dNTPs, 0.5µL Phusion®, 4µL appropriate primer pair, and 1µL of either BW25113 (promoters) or p3174 plasmid gDNA. Annealing temperature was set to 58°C, and the reaction was run for 35 cycles. Optimization using gradient PCR was required for amplification of the *arnB* promoter region. Following successful amplification, all PCR products were purified as described above, and one last PCR was completed in order to fuse the promoter and GFP regions together. This was also a 50µL reaction, and included: 27.5 MQ-H_2O, 10µL HF buffer, 2µL dNTPs, 0.5µL Phusion®, 4µL appropriate primer pair, and 3µL of each respective purified promoter and purified GFP product as the gDNA. All PCRs were verified using a 1% agarose gel, as described above. Subsequently, all products were purified as described above.

Table 4. Primers designed for amplification of GFP and *arnB*, *pagP*, *pmrD* promoters.

PRIMER	SEQUENCE
ArnB-Forward -P1	GAATCCGTAAACTCCACCTATAGACAAGCGC
ArnB-Reverse -P2	AGTTCTTCTCCTTTACGCATTGCTTTTCCTTCCGCCATTG
ArnB-GFP-Foward-P3	CAATGGCGGAAGGAAAAGCAATGCGTAAAGGAGAAGAACT
ArnB-GFP-Reverse-P4	AAGCTTTTATTTGTATAGTTCATCCATG
PagP-Forward-P1	GAATCCCCCAATAAATTGGCGATG
PagP-Reverse-P2	AGTTCTTCTCCTTTACGCATTTGTGACCATAAAACATTTATCAAAAATC
PagP-GFP-Forward-P3	GATTTTTGATAAATGTTTTATGGTCACAAATGCGTAAAGGAGAAGAACT
PagP-GFP-Reverse-P4	AAGCTTTTATTTGTATAGTTCATCCATG
PmrD-Forward-P1	GAATCCTCAGGCGCTAAAAGAGTGGG
PmrD-Reverse-P2	AGTTCTTCTCCTTTACGCATTGCATTATCCTGTTTGCTAAG
PmrD-GFP-Forward-P3	CTTAGCAAACAGGATAATGCAATGCGTAAAGGAGAAGAACT
PmrD-GFP-Reverse-P4	AAGCTTTTATTTGTATAGTTCATCCATG

*****Underlined sequence refers to restriction sites

3.13. Cloning purified *arnB*, *pagP* and *pmrD* promoter fusions with GFP into pCR2.1 TOPO Vector

After the SOE-PCR protocol, identical steps were taken to clone the fusion constructs into the pCR2.1 TOPO vector. A concise summary is as follows: 1) T-tailing of fusion constructs prior to cloning into pCR2.1 TOPO; 2) cloning into the vector; 3) transform cloned vectors into MACH1 cells using the heat shock protocol; 4) X-gal screening for blue and white colonies; 5) overnight subculture of white colonies; 6) plasmid extraction from subculture; 7) EcoRI double

digest of plasmid and sequence verification. The *pagP*-GFP fusion construct was unable to be produced. Therefore, we opted to use another PhoPQ regulated gene, *ompT*-GFP, of which we already had the construct made using the exact same protocol listed above.

3.14. Transformation of *arnB*, *ompT* and *pmrD*-GFP constructs into a panel of 8 clinical CD isolates using electroporation

Electrocompetent cells were prepared using ice-cold deionized water washes, for a total of four washes. Electrocompetent cells were aseptically moved into prechilled cuvettes with each respective construct, for a total of 24 strains (8 x each construct). Using the Bio-Rad GenePusler Xcell machine, cells were electroporated at 2.5V, followed by immediate addition of S.O.C. media for recovery. Subsequently, cells were recovered for 2 hours in a shaking 37°C incubator. After recovery time, cells were plated on LB agar + kanamycin plates at two concentration, 50µL and 200µL. The following day, successful plates were chosen, and colonies were picked to be sub-cultured in LB broth + kanamycin. If growth persisted the following day, freezer stocks were made for the respective strain.

3.15. Fluorescence assay monitoring gene induction in panel of 8 clinical CD isolates

Strains grown overnight are washed in HEPES buffer twice to assure no component of overnight media are carried over into the experiment. After washes, OD_{600} measurements are taken before assembling the plate. GFP assays were performed using black-well, clear bottom 96-well plates. To reduce error due to evaporation, the outer perimeter of the plate was filled with 225µL sterile dH_2O, which allows for insulation of the media inside. Two media conditions were tested per strain depending on the TCS construct. For *ompT*-GFP and *pmrD*-GFP, high magnesium (10mM) and low magnesium (20µM) M9 minimal media was used. For *arnB*-GFP, high iron (100µM) and low iron (0-10µM) M9 minimal media was used. In addition, to investigate a potential threshold concentration for stimulus of the PhoPQ system, a titration of Mg^{2+} concentrations were used. The concentrations used were: 20µM, 50µM, 100µM, 500µM, 1mM, 2mM, 5mM and 10mM. All strains were normalized to an OD_{600} reading of 0.1 and inoculated into wells that resulted in a final volume of 225µL (this included culture, media, and

antibiotic). Following plate preparation, a Biotek Synergy HTX Multi-Mode Reader was used to measure fluorescence and bacterial growth for 16.5 hours, taking reads for both fluorescence and OD_{600} every 30 minutes. The system was configured with an excitation wavelength of 485nm and emission wavelength of 530nm for appropriate fluorescent readouts. A total of three technical replicates and six biological replicates were performed. Please refer to Figure 6 a visual representation of a typical plate layout.

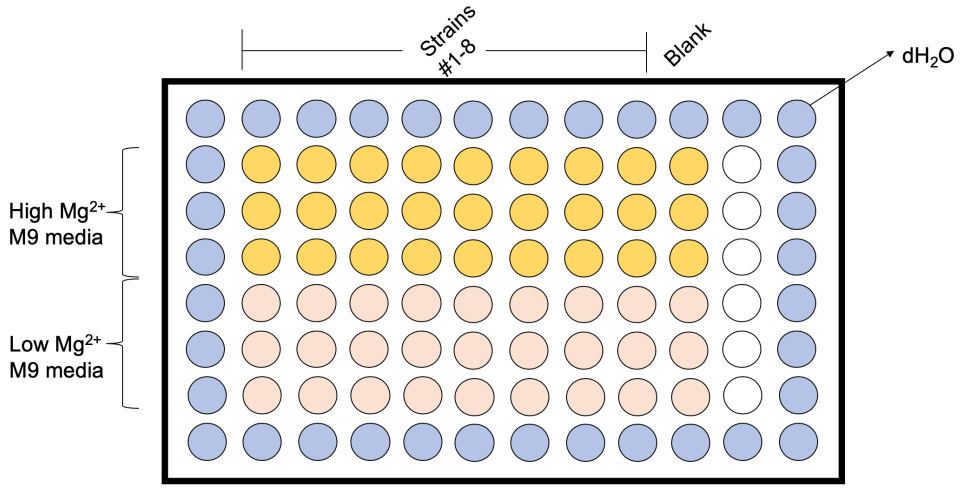

Figure 6. Example of 96-well plate layout for fluorescence assay testing for the PhoPQ TCS induction.

3.16. Polymyxin B killing assay

Killing assays were performed on the panel of 8 clinical CD isolates and a K12 strain to examine whether there are phenotypic changes associated with any altered signaling level. For killing assays, wild type CD isolates strains were grown overnight (without the GFP constructs). The following day, strains were washed once in HEPES buffer, and sub-cultured in high and low magnesium (10mM, 20μM respectively) M9 minimal media. The strains were grown to mid-log (OD_{600} ~0.6-0.8), at which point the cultured was washed in HEPES buffer one more time. After second HEPES wash, OD_{600} measurements were taken again. These OD_{600} readings were used to calculate how much of the culture was needed to reach a final concentration of 10^8 CFU/ml. After calculation, all strains + conditions were normalized to 10^8 CFU/ml. Normalized cells were subject to treatment with phosphate buffer saline (PBS) as a control, and various concentrations of polymyxin B (PMB) treatment. For the CD isolates, seven concentrations of polymyxin B

were used; 1µg/ml, 2µg/ml, 5µg/ml, 10µg/ml, 25µg/ml, 50µg/ml and 100µg/ml. For K12, a lower range of polymyxin B was used; 0.1µg/ml, 0.2µg/ml, 0.5µg/ml, 1µg/ml, 2µg/ml, and 5µg/ml. Both control and polymyxin treated cells were transferred to titer tubes containing PBS to stop further killing from occurring at two time points, 0 minutes and 10 minutes. 2µL culture samples were taken and diluted 1:250 (10^0) in PBS and further diluted 1:10 to generate 10^{-1}. 10 µL samples of both dilutions were spot plated on LB agar plates and incubated at room temperature overnight until colonies could be counted. Minimum of four biological replicates were performed for each strain/condition and colony counts were the sum of four technical plating replicates.

3.17. Construction of PhoP-HA-tag

To monitor PhoP translation and phosphorylation via western blot analysis, HA was tagged to PhoP. Primers were designed to amplify PhoP, with the reverse primer containing the HA sequence to efficiently tag the C-terminus of PhoP (**Table. 5**). Similar protocols mentioned above were followed. A concise summary is as follows: 1) PCR amplification; 2) cloning into TOPO blunt vector; 3) transform cloned vectors into DH5a cells using the heat shock protocol; 4) X-gal screening for blue and white colonies; 5) overnight subculture of white colonies; 6) plasmid extraction from subculture; 7) EcoRI double digest of plasmid and sequence verification. Following sequence verification, constructs were subcloned into a low-copy plasmid pWSK129 using similar protocols as mentioned above. Once subcloning was verified, constructs were transformed into the panel of 8 electrocompetent CD isolates and K12 using the electroporation method.

Table 5. Primers designed for amplification of PhoP-HA-tag.

PRIMER	SEQUENCE
PhoP-Forward	GAATCCTTGGTCGAGCTATCACGATG
PhoP-Reverse	AAGCTTTCAAGCGTAATCTGGAACATCGTATGGGTAGCGCAATTCGAACAG

*Underlined sequence refers to restriction sites
*Blue refers to HA sequence

3.18. Subpopulation analysis

A BD Accuri™ C6 Plus Flow Cytometer was used to observe the populations dynamic of all relevant strains at a single-cell level. Strains which contained the *pmrD*-GFP fusion were grown overnight in either low Mg^{2+} (20μM) or high Mg^{2+} (10mM) M9 media. The following day, cultures were washed once in 1X PBS. After the first wash, the cultures were centrifuged, and the supernatant was removed. Following this, cells were resuspended in approximately 100μL of 1X PBS and then mixed with 1mL of 1:1 methanol acetone for fixing of cells. At this point the cells were incubated at room temperature for 10-15 minutes. After incubation, cells were centrifuged, the supernatant was completely removed, and cells were resuspended in 1mL 1X PBS. The samples were run through the Flow Cytometer for single-cell analysis. The parameters used for differentiating inducing and non-induced populations were FITC-A (detecting green fluorescence), and FSC-A (detecting forward scatter). 10,000 cells were counted for each strain + condition (18 total samples).

4. Results

4.1. Differential regulation of *pmrD* and *ompT* are observed in divergent strains of IBDEC

Based on previous data collected from Youn Hee Cho and Michael Renouf which highlighted variation in resistance phenotypes of clinical IBDEC isolates to HDPs LL-37 and hBD3, we hypothesized that the altered signaling levels of downstream genes involved in HDP resistance could explain the observed pattern (Unpublished, Cho, Renouf and McPhee). To test this, we created reporter genes for PhoPQ signaling. We chose two PhoPQ regulated genes, *pmrD* for its role in connecting to the PmrAB TCS, the master regulator of LPS modifications, and *ompT*, a protease capable of cleaving HDP LL-37 (Unpublished, Cho, Fadle, and McPhee). We fused the promoter regions of these genes from a K12 strain, BW25113, to GFPmut3 and cloned the fused product into the pCR2.1 TOPO vector. We selected a panel of eight CD clinical isolates to conduct our reporter experiments. Strains were selected based on meeting one of four criteria: 1) have high level resistance to both LL-37 and hBD3, 2) have low level resistance to LL-37 and hBD3, 3) have high level resistance to LL-37 and low level resistance to hBD3, and 4) have low level resistance to LL-37 and high level resistance to hBD3. Of our eight selected strains, two belonged to each one of the criteria (**Table. 6**).

Table 6. Resistance profiles of selected clinical isolates against HDPs LL-37 and hBD3.

Strain	LL-37 resistance (%)	hBD3 resistance (%)	Resistance group LL37/hBD3
DK3	0.74%	2.22%	Low/Low
DK26	0.80%	1.92%	Low/Low
DK89	0.69%	80.26%	Low/High
DK136	79.36%	75.87%	High/High
DK236	75.12%	0.08%	High/Low
UM146	106.55%	86.99%	High/High
DF-06	1.68%	106.15%	Low/High
PP-26	140.44%	46.80%	High/Low

To measure PhoPQ signaling, we conducted overnight experiments measuring the promoter activity of each construct in K12 and the selected CD isolates. To repress and induce PhoPQ, we used high (10mM) and low (20µM) magnesium M9 minimal media respectively during the experiment. As expected, we saw significantly altered signaling levels in both non-inducing and inducing conditions for the *pmrD*-GFP and *ompT*-GFP constructs in our panel of CD isolates (**Fig. 7**). While there are numerous ways to analyze this data set, we initially focused on measuring the difference of induced PhoPQ signaling of our clinical isolates to our K12 strain. Of particular interest were two IBDEC strains, DK89 and UM146. DK89, a CD isolate with high resistance to hBD3 and low resistance to LL-37, was one of the highest *pmrD* signaling strains we tested. Interestingly, when measuring *ompT* signaling in this background, we found DK89 had one of the lowest expressions among the all strains tested. UM146, on the hand, showed the exact opposite, where it was the lowest *pmrD* signaling strains, but the highest *ompT* signaling strain among the clinical CD strains. When compared to a K12 strain, there is consistently a lower and tightly regulated fold-change between non-inducing to inducing conditions. For instance, for *pmrD*, all CD isolates hover tightly around a 2-fold change, while the K12 strain exhibits a 5-fold change from non-inducing to inducing conditions (**Fig. 7 b**).

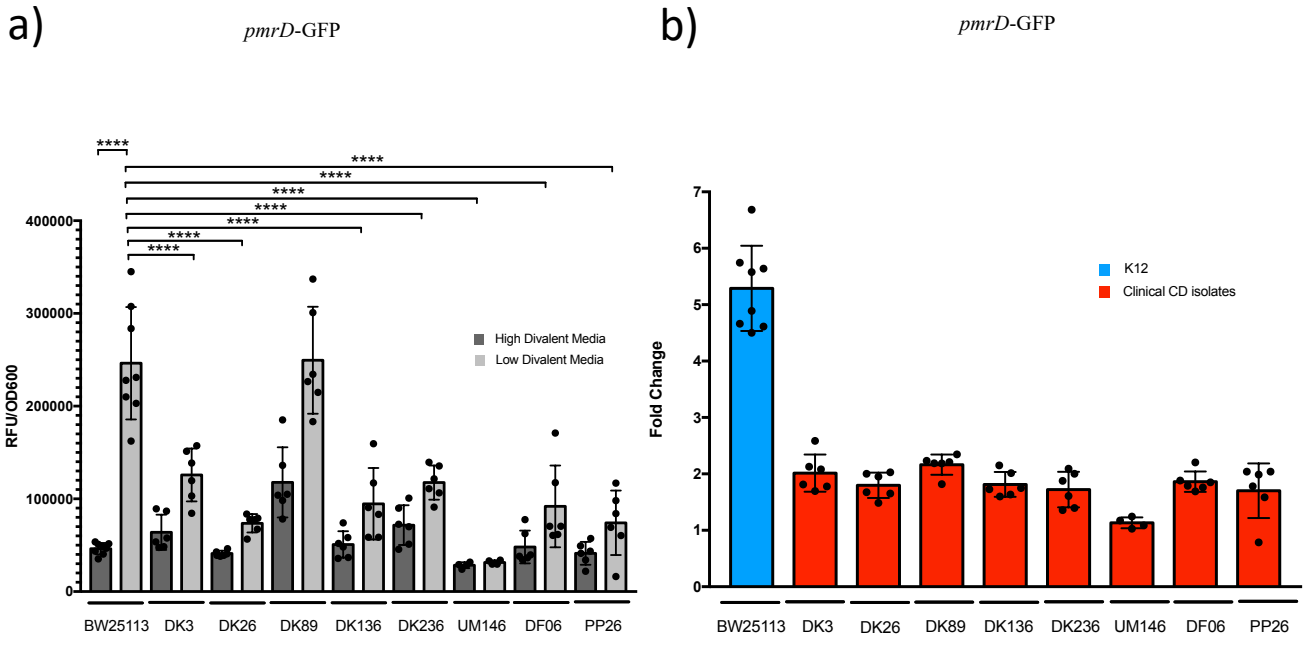

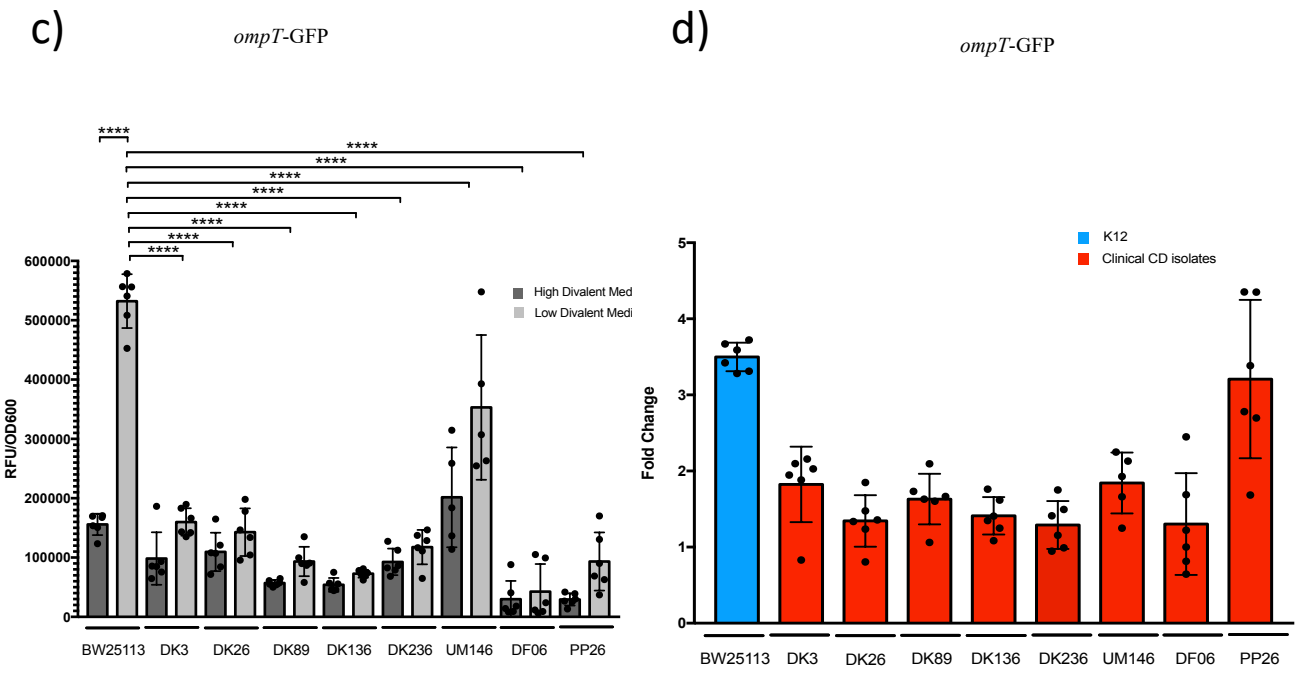

Figure 7. Measuring PhoPQ signaling in K12 and CD isolates under fixed Mg^{2+} concentrations.

a) Expression from a *pmrD*-GFP fusion construct in different clinical CD isolates grown in M9 minimal medium containing PhoP-inducing levels of Mg^{2+} (20µM) or PhoP-repressing levels of Mg^{2+} (10mM). b) Relative fold change in *pmrD*-GFP expression from non-inducing to inducing conditions. c) Expression from an *ompT*-GFP fusion construct in the same clinical isolates and media. d) Relative fold change in *pmrD*-GFP expression from non-inducing to inducing conditions. Compared to WT K12 strain of *E. coli* (BW25113), majority of clinical isolates of AIEC exhibit differential regulation of genes associated with HDP resistance (* $p<0.05$; *** $p<0.001$; **** $p<0.0001$). Each dot represents one biological replicate.

4.2. Strain-to-strain differences in the relationship between Mg^{2+} concentrations and PhoPQ signaling

While induction of the PhoPQ system under limiting magnesium conditions is well established, to date there has not been much insight of the systems response to a gradient of magnesium conditions. Given the differences in the absolute signaling potential between our IBDEC strains, we wanted to test how these strains respond to increasing concentrations of Mg^{2+} to elucidate a potential strain-specific inducing threshold concentration of Mg^{2+} for PhoPQ activation. To assess this, we completed fluorescence assays using the *pmrD*-GFP construct exposed to eight different increasing concentrations of magnesium in M9 minimal media. Our selected Mg^{2+} concentration gradient for these experiments was 20µM, 50µM, 100µM, 500µM, 1mM, 2mM, 5mM and 10mM.

Our results confirmed the inverse relationship between Mg^{2+} concentration and PhoPQ activation, consistent with literature and previous experiments. However, while all strains follow the same general pattern, long-term response to the Mg^{2+} differs substantially from strain-to-strain. For instance, in our K12 strain, we see an exponential signaling response to Mg^{2+} concentrations (**Fig. 8 b**), while strain DK89 exhibits a relatively consistent signaling output throughout all concentrations (**Fig. 8 e**). Another interesting observation was the potential of strains DK3, DK26, DK136 and DF-06 to respond robustly to our lowest, most inducing concentration of Mg^{2+}, and then show a steep decline in *pmrD* expression when cultured in higher Mg^{+} concentrations (**Fig. 8 c, d, f and j**). This phenomenon might reflect differences in PhoPQ sensitivity in these strain to an inducing stimulus. To view the signaling data on the same figure, we plotted the average of the peak expression from each strain at each concentration of Mg^{2+} (**Fig. 8 a**).

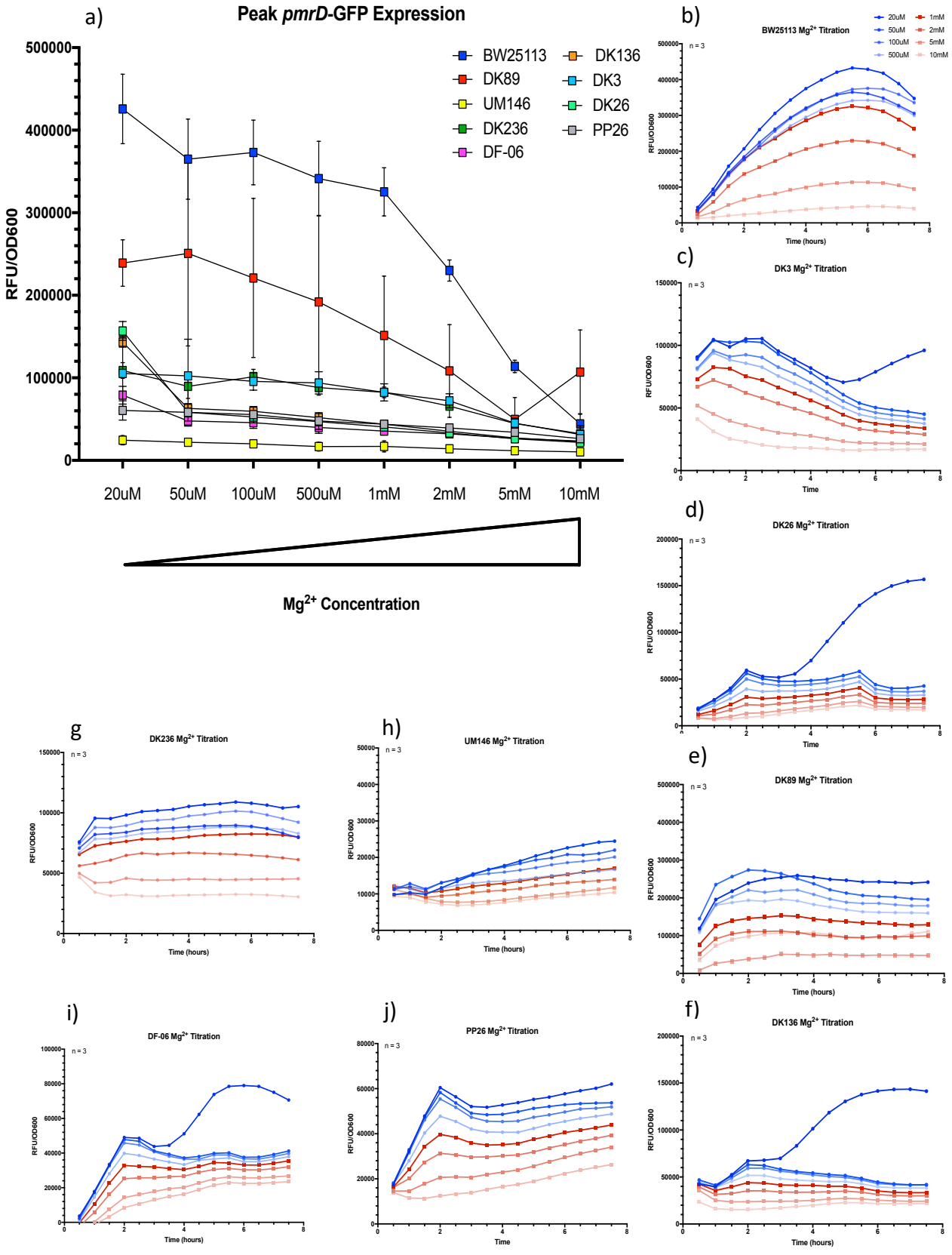
a)
Peak pmrD-GFP Expression
BW25113
DK89
UM146
DK236
DF-06
DK136
DK3
DK26
PP26
RFU/OD600
20uM
50uM
100uM
500uM
1mM
2mM
5mM
10mM
Mg2+ Concentration
b)
BW25113 Mg2+ Titration
c)
DK3 Mg2+ Titration
d)
DK26 Mg2+ Titration
e)
DK89 Mg2+ Titration
f)
DK136 Mg2+ Titration
g
DK236 Mg2+ Titration
h)
UM146 Mg2+ Titration
i)
DF-06 Mg2+ Titration
j)
PP26 Mg2+ Titration
Time (hours)
n = 3

Figure 8. PhoPQ signaling response to increasing Mg^{2+} concentrations.

a) Snapshot of peak *pmrD*-GFP expression at set concentrations of Mg^{2+} in the panel of CD isolates and K12. b-j) Kinetic expression of *pmrD*-GFP in all relevant strains when exposed to increasing concentrations of Mg^{2+}; data points represent the average of 3 biological replicates.

4.3. PMB resistance of IBDEC strains differs due PhoPQ signaling potential

To assess if there are phenotypic differences associated with the altered signaling levels among strains, we performed polymyxin B killing assays to analyze if signaling potential can predict bacterial resistance. To test this, we challenged our panel of isolates with increasing concentrations of drug to uncover strain-to-strain differences in resistance. In this model, we would predict that a high PhoPQ signaling strain would result in resistance at higher concentrations of PMB. In addition, we also wanted to establish that resistance phenotypes change when bacteria are cultured in non-inducing vs. inducing media. Here, we would predict the resistance of strains will be greater when cultured in PhoPQ inducing media (20μM M9) vs. being cultured in non-inducing media (10mM M9). The concentrations we chose to test were 1μg/ml, 2μg/ml, 5μg/ml, 10μg/ml, 25μg/ml, 50μg/ml and 100μg/ml for our clinical isolates, and 0.1μg/ml, 0.2μg/ml, 0.5μg/ml, 1μg/ml, 2μg/ml, and 5μg/ml for our K12 strain.

We found the resistance patterns of some strains align with the altered signaling levels for each respective strain. For instance, DK89, a clinical isolate that exhibited the most absolute induction of *pmrD* shows the highest resistance profile and substantial difference in resistance phenotypes when grown in either inducing or non-inducing conditions (**Fig. 9 d**). Other strains, on the other hand, show a rather surprising phenotype of elevated resistance when grown in non-inducing media vs. inducing media. For example, strains DK26 and DK236, both of which had low to medium level of *pmrD* induction, appear to be more resistant in non-inducing conditions. This observation is also noted in the K12 background, where we see higher levels of resistance when cultured in non-inducing media. We want to investigate potential explanations for some of the observations seen here by conducting single-cell analysis, inductively coupled plasma (ICP) analysis looking at Mg^{2+} sequestration by the strains, screening for resistance sub-populations among isogenic cultures, and also sequencing the genomes.

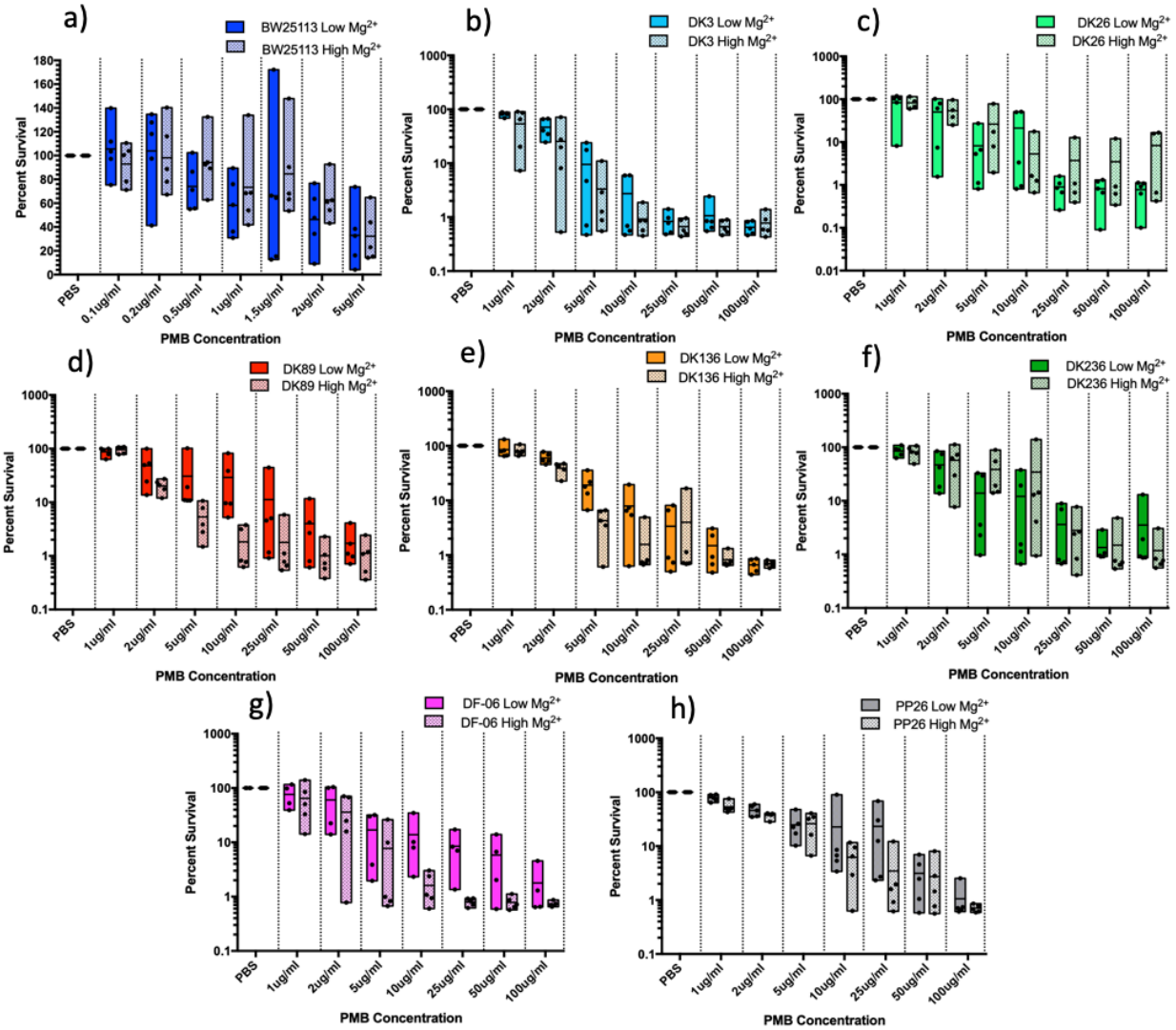

Figure 9. Polymyxin B resistance of K12 and CD isolates to increasing drug concentrations.

a-h.) Resistance of K12 clinical CD isolates to seven concentrations of polymyxin B shows phenotypic differences among each strain when grown in inducing (20μM Mg^{2+}) or non-inducing conditions (10mM Mg^{2+}). Each dot represents one biological replicate. Boxes represent spread of data (minimum to maximum).

4.4. PmrA transcriptional feedback repression results in reduced *pmrD* expression in IBDEC strain DK89

Upregulation of *pmrD* results in the induction of PmrA-activated genes under Fe^{3+} replete conditions. Previous work by Kato *et. al* in 2003 showed that the PmrA protein footprinted on the *pmrD* promoter, therefore giving evidence of direct regulation of *pmrD* by PmrA post transcriptionally[65]. This interaction occurs when the PmrAB system is activated independently

from the PhoPQ system. Therefore, we wanted to determine if under PmrA inducing conditions via PmrB (high Fe^{3+}) we saw repression of the *pmrD*-GFP construct in our panel of selected strains. To do this, we conducted a fluorescence assays measuring *pmrD* expression using two minimal media types, low Mg^{2+} (20μM), and low Mg^{2+} (20μM) + high Fe^{3+} (100μM). Here, we see that strain DK89, a highly induced strain, seems to have active repression of *pmrD* under PmrAB inducing conditions (**Fig. 10**).

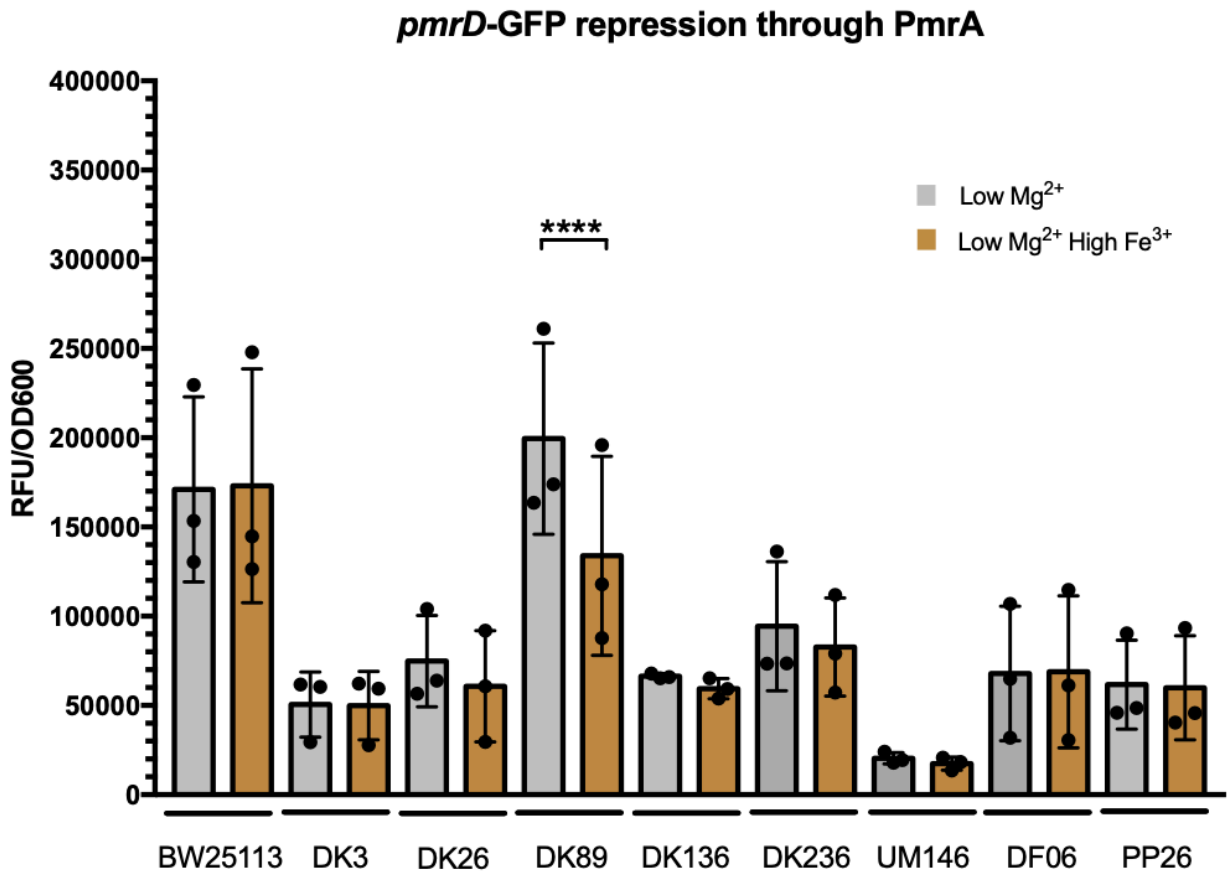

Figure 10. *pmrD* repression through the PmrAB TCS.

Expression from a *pmrD*-GFP fusion construct in K12 and CD isolates grown in M9 minimal medium containing PhoPQ-inducing levels of Mg^{2+} (20μM) or PhoPQ and PmrAB induing conditions, low Mg^{2+} (20μM) + high Fe^{3+} (100μM). (**** $p<0.0001$). Each dot represents one biological replicate. Error bars represent standard deviation.

4.5. Differential *pmrD* and *ompT* signaling in other pathogenic *E. coli strains*

Due to the observed heterogeneity in signaling levels downstream of the PhoPQ TCS in a subset of IBDEC, we probed the question whether a same trend could be seen in other pathogen strains of *E. coli*. We chose to screen four well-characterized pathogenic strains of *E. coli*: EHEC strains DK O157:H7 and 86-24, UPEC strain NU-14, and EPEC strain E2348/64. To monitor PhoPQ signaling in these strains, we used both of our *ompT*-GFP and *pmrD*-GFP constructs to perform fluorescence assays to measure the induction of these genes. The same parameters were used as mentioned above, where we measured signaling in both PhoPQ repressing (10mM Mg^{2+}) and inducing (20μM Mg^{2+}) M9 media.

Highly virulent EHEC strain O157:H7 exhibited a high and robust level of induction for both *ompT* and *pmrD*, irrespective of whether inducing or non-inducing media was used (**Fig. 11**). In fact, PhoPQ signaling under non-inducing conditions for O157:H7 rivaled the induced signaling of our highest *pmrD* signaling strain DK89. In addition, there was a slight fold-change in both *ompT* and *pmrD* expression from non-inducing to inducing conditions in this EHEC background. Therefore, we sought to address whether regulation of both *ompT* and *pmrD* was still PhoPQ dependent in EHEC. To test for this, we conducted the same experiment using another EHEC strain called 86-24, where we had a PhoP KO in the same background. Firstly, we wanted to establish the same signaling trend in this EHEC background. Albeit to a much lower magnitude, EHEC strain 86-24 also shows small to no differences in signaling when cultured in non-inducing vs. inducing conditions. However, when we used a PhoP KO in this background, we saw complete loss of signaling of both *ompT* and *pmrD*, suggesting that gene expression is still contingent upon PhoPQ signaling despite the low fold change between inducing and non-inducing conditions. While strains UPEC NU-14 and EPEC E2348/64 showed lower overall induction of *ompT* compared to O157:H7, the fold change between non-inducing and inducing conditions was higher (~2 fold). Interestingly, strains UPEC NU-14 and EPEC E2348/64 showed little induction of *pmrD*, with almost no difference in fold change between inducing and non-inducing conditions. These observations highlight two things, 1) the altered PhoPQ signaling between IBDEC strains also occurs between different strains of EHEC, and 2) despite both being

regulated by PhoPQ, *ompT* and *pmrD* show different levels of signaling under identical conditions.

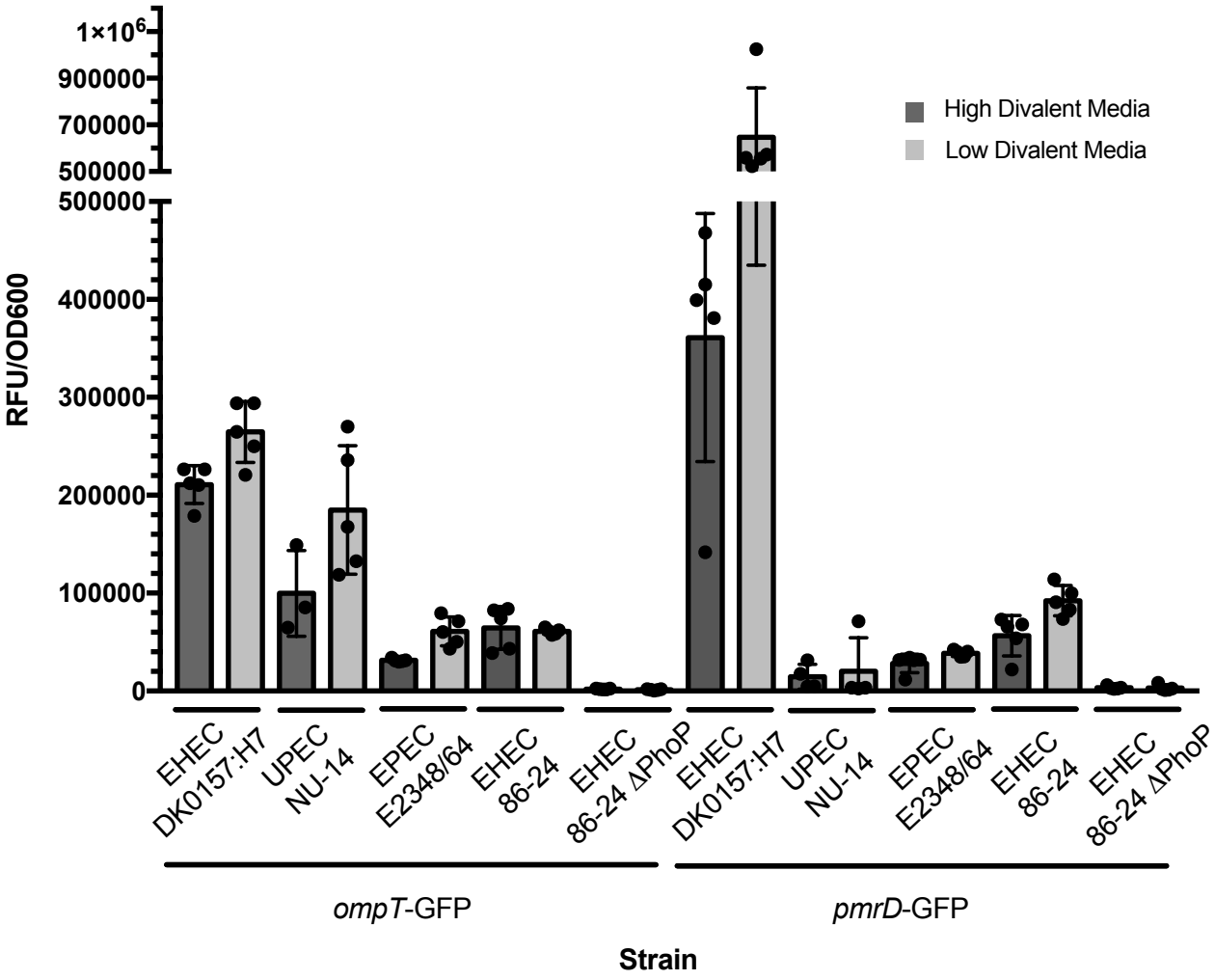

Figure 11. PhoPQ signaling in non-IBDEC pathovars of *E. coli*.

Expression from the *ompT* and *pmrD*-GFP fusion construct in clinical isolates of EHEC DK O157:H7, UPEC isolate NU-14, EPEC E2348/64, EHEC 86-24, and EHEC 86-24 with a PhoP KO. All strains were grown in M9 minimal medium containing PhoP-inducing levels of Mg^{2+} (20μM) or PhoP-repressing levels of Mg^{2+} (10mM). Each dot represents one biological replicate. Error bars represent standard deviation.

4.6. Subpopulation analysis highlights differential signaling potential and morphology among IBDEC strains

Given the broad range of PMB resistance phenotypes observed, we wanted to analyze the strains at a single-cell level to uncover any insight into heterogeneity within isogenic cultures that might be driving the population dynamics as a whole[66]. The end product of our PMB killing assays select for cells that survived exposure to a set concentration of drug. What can go unnoticed in these experiments is a subpopulation of resistant cells within an isogenic culture that could be pushing the resistance phenotypes we measure. For instance, strains that showed higher resistance to PMB when cultured in PhoPQ repressing media vs. inducing media could have a large portion of intrinsically resistant cells. Therefore, when we measure PMB resistance of these strains, we are also indirectly measuring potentially hetero-resistant subpopulations within the strains (**Fig. 12**). This phenomenon, called heteroresistance or heterogenous resistance, is emerging topic in the field of microbiology.

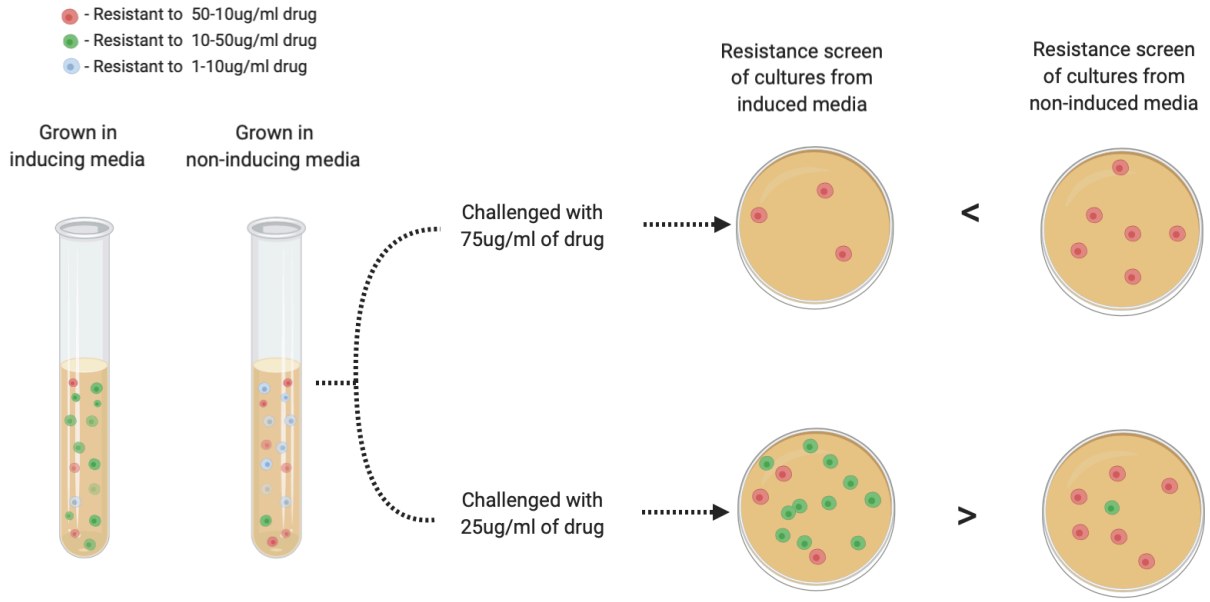

Figure 12. Heteroresistance within isogenic cultures.

An example of heteroresistance within the same strain grown in either inducing or non-inducing media. Blue, green, and red cells depict subpopulations of bacterial cells from an isogenic culture with different resistance to an antimicrobial drug. While the induced population might have an overall higher resistance profile at a fixed concentration (left culture), the un-induced population may contain more hetero-resistant subpopulations that can lead to higher resistance to a higher concentration of drug (right culture).

To assess the heteroresistance profiles of our selected strains, we used flow cytometry to measure *pmrD*-GFP activity. We grew all our strains overnight in either PhoPQ inducing (20µM Mg^{2+}) or PhoPQ repressing (10mM Mg^{2+}) M9 media. The following day, we fixed the cells, and resuspended the cultures in PBS, after which they were run through the flow cytometer to measure two primary parameters; green fluorescence and forward scatter. According to our PMB killing data, we would predict that strains which showed higher resistance when cultured in non-inducing media would have a larger spread in *pmrD* signaling (e.g. GFP signal intensity) that overlaps with the induced cultures. As a whole, the results from this experiment support our previous data showing up-regulation of *pmrD* expression in PhoPQ inducing conditions when compared to PhoPQ repressing conditions. Additionally, we found strains to differ in their spread of *pmrD*-GFP activation in either media condition. For instance, strains DK236 and DK136 show tight and distinct clustering of cells for either media condition, while strains DF-06 and DK3 show more variability in the spread of data with quite a lot of overlap between the two media types. Interestingly, there seems to be a relationship between non-induced cells with higher forward scatter, which for our purposes represents bacterial cell size. This suggests that a potential downstream target of PhoPQ system is/are gene(s) associated with altering overall cell morphology.

a)

	Sample Name	Subset Name	Count
	A09 BW25113 L.fcs	Ungated	10000
	B09 BW25113 H.fcs	Ungated	10000

Strain: BW25113			
Low Mg2+		High Mg2+	
Mean (GFP)	13709	Mean (GFP)	548
Mean (FSC)	149723	Mean (FSC)	48500
Median (GFP)	6224	Median (GFP)	189
Median (FSC)	129745	Median (FSC)	128251
Robust CV (GFP)	169	Robust CV (GFP)	316
Robust CV (FSC)	49.4	Robust CV (FSC)	48.2

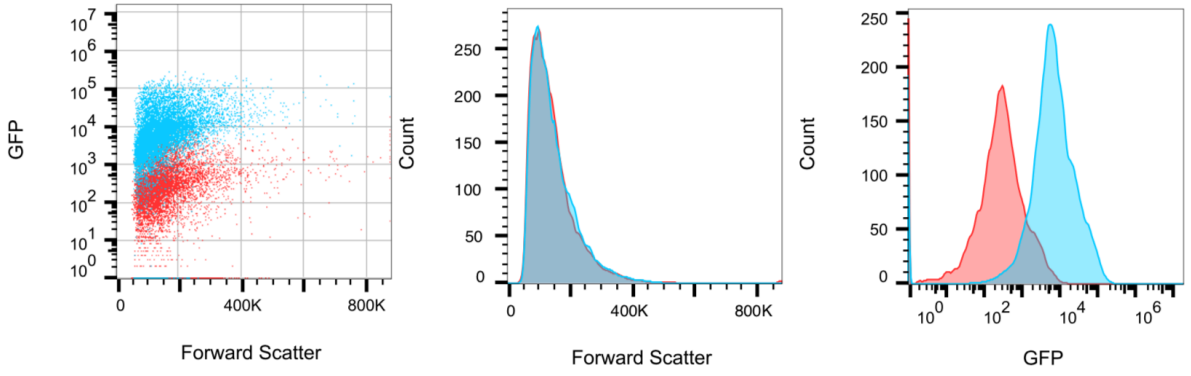

b)

	Sample Name	Subset Name	Count
	A03 DK89 L.fcs	Ungated	10000
	B03 DK89 H.fcs	Ungated	10000

Strain: DK89			
Low Mg2+		High Mg2+	
Mean (GFP)	4147	Mean (GFP)	323
Mean (FSC)	114348	Mean (FSC)	141514
Median (GFP)	2209	Median (GFP)	149
Median (FSC)	95815	Median (FSC)	121422
Robust CV (GFP)	107	Robust CV (GFP)	249
Robust CV (FSC)	38.6	Robust CV (FSC)	44.4

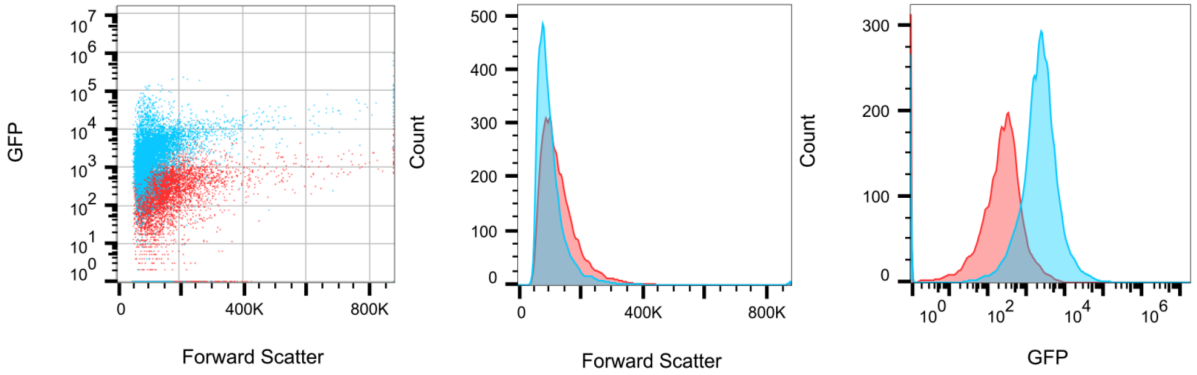

c)

	Sample Name	Subset Name	Count
	A06 UM146 L.fcs	Ungated	10000
	B06 UM146 H.fcs	Ungated	10000

Strain: UM146			
Low Mg2+		High Mg2+	
Mean (GFP)	846	Mean (GFP)	225
Mean (FSC)	115551	Mean (FSC)	169411
Median (GFP)	238	Median (GFP)	94.1
Median (FSC)	88773	Median (FSC)	89413
Robust CV (GFP)	226	Robust CV (GFP)	136
Robust CV (FSC)	40.4	Robust CV (FSC)	107

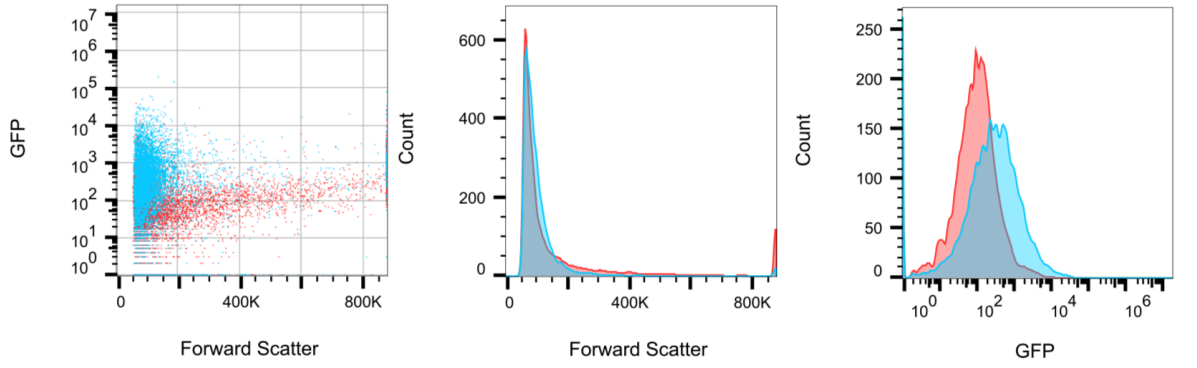

d)

	Sample Name	Subset Name	Count
	A05 DK236 L.fcs	Ungated	10000
	B05 DK236 H.fcs	Ungated	10000

Strain: DK236			
Low Mg2+		High Mg2+	
Mean (GFP)	54671	Mean (GFP)	1086
Mean (FSC)	134364	Mean (FSC)	185173
Median (GFP)	49385	Median (GFP)	400
Median (FSC)	124197	Median (FSC)	158980
Robust CV (GFP)	59.9	Robust CV (GFP)	258
Robust CV (FSC)	36.1	Robust CV (FSC)	50.1

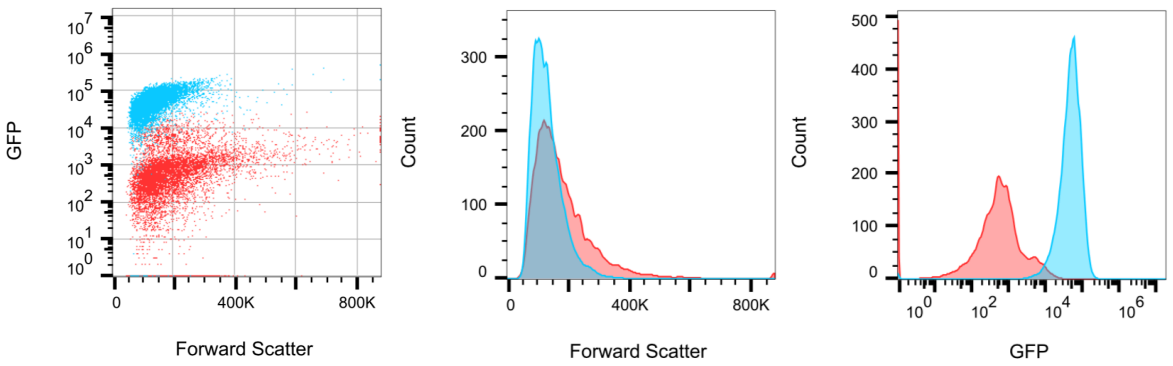

e)

	Sample Name	Subset Name	Count
	A07 DF-06 L.fcs	Ungated	10000
	B07 DF-06 H.fcs	Ungated	10000

Strain: DF-06			
Low Mg2+		High Mg2+	
Mean (GFP)	2522	Mean (GFP)	256
Mean (FSC)	145739	Mean (FSC)	155841
Median (GFP)	794	Median (GFP)	147
Median (FSC)	132946	Median (FSC)	141908
Robust CV (GFP)	517	Robust CV (GFP)	229
Robust CV (FSC)	38.5	Robust CV (FSC)	42.7

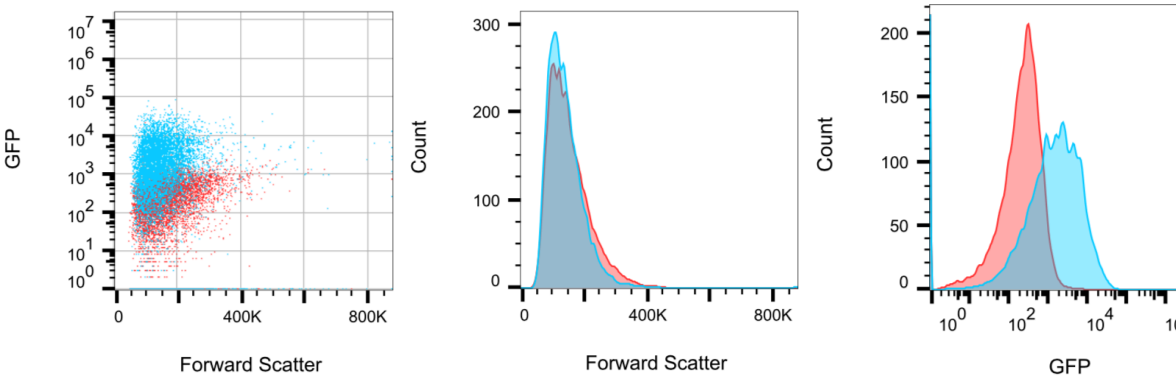

f)

	Sample Name	Subset Name	Count
	A04 DK136 L.fcs	Ungated	10000
	B04 DK136 H.fcs	Ungated	10000

Strain: DK136			
Low Mg2+		High Mg2+	
Mean (GFP)	18925	Mean (GFP)	800
Mean (FSC)	137392	Mean (FSC)	169616
Median (GFP)	17319	Median (GFP)	500
Median (FSC)	126757	Median (FSC)	152151
Robust CV (GFP)	56.6	Robust CV (GFP)	201
Robust CV (FSC)	36.1	Robust CV (FSC)	47

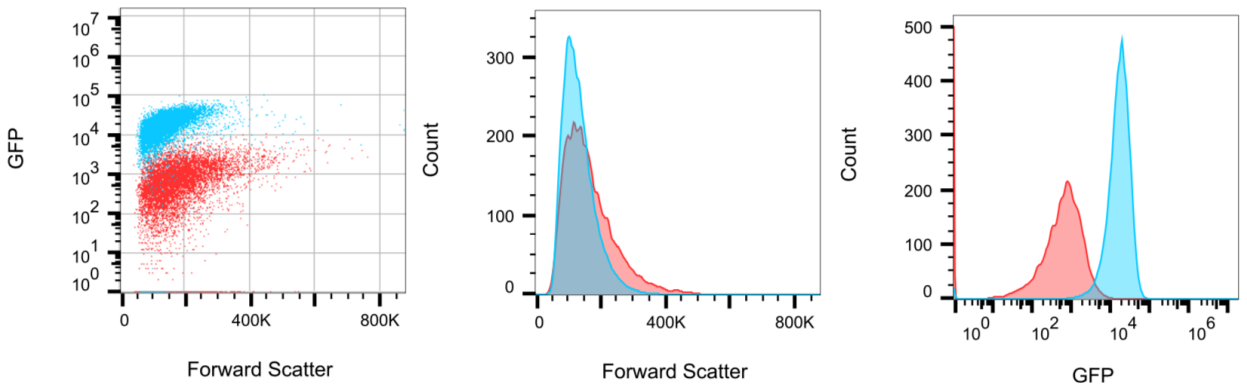

g)

	Sample Name	Subset Name	Count
	A01 DK3 L.fcs	Ungated	10000
	B01 DK3 H.fcs	Ungated	10000

Strain: DK3			
Low Mg2+		High Mg2+	
Mean (GFP)	21752	Mean (GFP)	780
Mean (FSC)	120320	Mean (FSC)	176813
Median (GFP)	11585	Median (GFP)	137
Median (FSC)	106912	Median (FSC)	151298
Robust CV (GFP)	169	Robust CV (GFP)	860
Robust CV (FSC)	37.5	Robust CV (FSC)	52

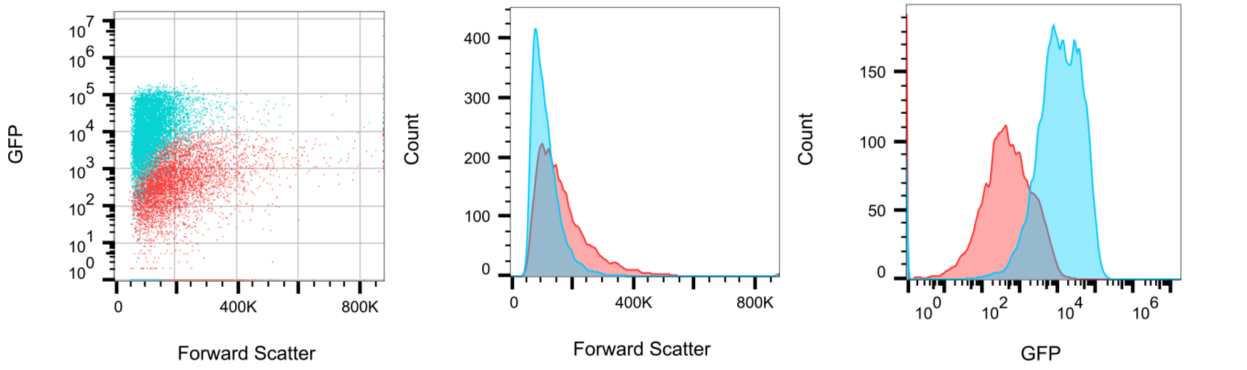

h)

	Sample Name	Subset Name	Count
	A02 DK26 L.fcs	Ungated	10000
	B02 DK26 H.fcs	Ungated	10000

Strain: DK26			
Low Mg2+		High Mg2+	
Mean (GFP)	14721	Mean (GFP)	323
Mean (FSC)	141107	Mean (FSC)	167426
Median (GFP)	12313	Median (GFP)	125
Median (FSC)	122276	Median (FSC)	149804
Robust CV (GFP)	81.8	Robust CV (GFP)	276
Robust CV (FSC)	39.4	Robust CV (FSC)	45.7

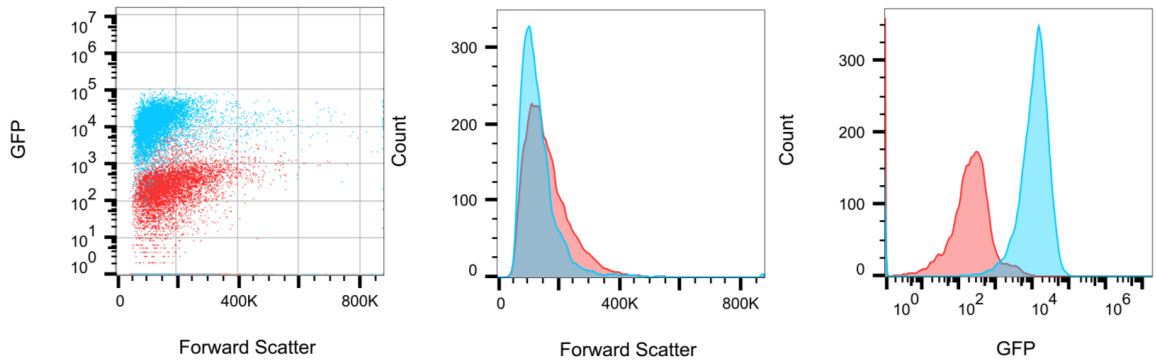

i)

	Sample Name	Subset Name	Count
	A08 PP26 L.fcs	Ungated	10000
	B08 PP26 H.fcs	Ungated	10000

Strain: PP26			
Low Mg2+		High Mg2+	
Mean (GFP)	596	Mean (GFP)	283
Mean (FSC)	255643	Mean (FSC)	261133
Median (GFP)	71.1	Median (GFP)	77.1
Median (FSC)	155352	Median (FSC)	153645
Robust CV (GFP)	572	Robust CV (GFP)	290
Robust CV (FSC)	123	Robust CV (FSC)	129

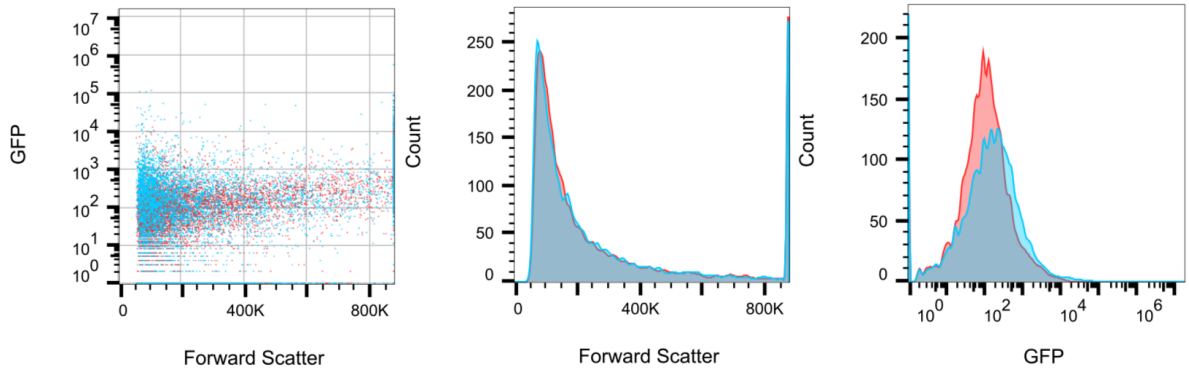

Figure 13. Single-cell analysis of *pmrD* expression and cell size.

a-i) Single-cell analysis of *pmrD*-GFP construct in K12 and CD isolates using a Flow Cytometer. Parameters shown are Forward Scatter (FSC) and GFP, with primary statistics being mean, median, and robust CV for both FSC and GFP. Strains were grown overnight in either low Mg^{2+} (20μM) or high Mg^{2+} (10mM) prior to fixing with 1:1 methanol acetone.

5. Discussion

IBD is complex, multifactorial disorder that affects 1 in 50 people in Canada[11]. While several treatment options exist for those that suffer from IBD, there is a need to better understand the etiology of this disease. The human gut microbiome, which plays a critical role in maintaining host health, is altered in those that suffer from either CD or UC[27]. Within this altered community is the increased prevalence IBDEC, a pathogen that has shown the ability to successfully colonize the HDP abundant epithelial surface of the gut[28,29,98]. IBDEC's survival against these peptides relies heavily on intricate bacterial signaling through conserved pathways that ultimately lead to increased expression of genes involved in cationic peptide resistance. Previous work in the McPhee lab has characterized disease specific HDP resistance among a large collection of IBDEC isolates. However, while resistance exists, there is large strain-to-strain variation in resistance phenotypes, ranging from completely susceptible to completely resistant. Here, we show evidence that this strain-to-strain variation is through differential PhoPQ signaling, a TCS critical for HDP resistance, in a panel of eight CD clinical isolates when induced using the same concentration of stimulus. Furthermore, the magnitude of strain-specific signaling might be used to predict the resistance profiles of these strains to cationic antimicrobial peptides.

To measure the transcriptional regulation of PhoPQ regulated genes, we sought to use a GFP reporter system. This system has been widely employed in *E. coli* models over the last two decades, with several different successful examples of studies looking at expression of genes involved in DNA repair, amino-acid synthesis pathways, flagella synthesis and much more[105]. Remarkable work from the Bren group in 2006 made significant progress at using this system in *E. coli* by making GFP transcriptional fusions to 75% of promoters found in the organism, creating a powerful resource for those exploring *E. coli* gene systems[105]. Our PhoPQ reporters included fusing the promoters of two PhoPQ regulated genes, *pmrD* and *ompT*, from a K12 strain BW25513 to GFP, bringing the transcription of GFP under the control of these promoters. We transformed these constructs into a K12 background and a panel of eight clinical CD isolates, where we induced or repressed the PhoPQ system and measured the activity of these promoters independently.

5.1. Heterogeneity in PhoPQ signaling among IBDEC isolates

Our work shows that there are significant differences in the expression of both *pmrD* and *ompT* under both PhoPQ inducing and repressing conditions among our clinical isolates (**Fig. 7**). While there are a number of ways to analyze this data set, we first opted to focus on looking at strain-to-strain differences in signaling when the system was induced using low Mg^{2+} minimal media (20μM). When we compared the induced signal from our CD isolates to our K12 control strain BW25113, we found, rather surprisingly, that BW25113 showed the highest signaling potential for both of our reporter genes. As these genes are involved in resistance to HDP, we anticipated the expression to be higher in our clinical isolates. The high signaling potential of BW25113 also correlated with a higher fold-change from non-inducing to inducing conditions (~5-fold for *pmrD* and ~3.5-fold for *ompT*) when compared to the clinical isolates (~2-fold for *pmrD* and ~1.7-fold for *ompT*).

5.1.1. IBDEC strains differ in long-term signaling dynamics

To study the intermediate dynamics of PhoPQ activation or repression, we used increasing concentrations of Mg^{2+} in our media to determine if we could reveal a strain-specific Mg^{2+} dependent threshold that switches PhoPQ from its repressive state to activating (**Fig. 8**). Consistent with our understanding of the PhoPQ system, all strains exhibited an inverse relationship between extracellular Mg^{2+} concentration and PhoPQ signaling. While we were not able to see an activation threshold for all of our strains, we were able to see interesting subtleties in the PhoPQ response in a subset of our strains. BW25113 showed significant response in signal as we transiently switch from repressive to inducing media. The biggest clustering of PhoPQ response we detected was at the 20μM to 1mM Mg^{2+} range, suggesting a possible activation threshold range in this K12 background (**Fig. 8b**). On the other hand, other clinically isolated strains had varied responses. For instance, strain DK89, our highest *pmrD* signaling strain, did not show exponential signaling potential over time, but rather a steady, plateaued signaling increase depending on the concentration (**Fig. 8e**). Strains DK3, DK26, DK136 and DF-06 respond well to the most inducing (lowest) concentrations of Mg^{2+} but have a steep decline in signaling at any Mg^{2+} concentrations greater than that (**Fig. 8 c, d, f, i**). This could be attributed

to one of two things, 1) lack of bacterial growth at the lowest Mg^{2+} concentration, or 2) a more robust response of these strains to the lowest Mg^{2+} concentration. In order to normalize for bacterial growth, we divide the fluorescence units generated from our reporter genes by the OD_{600}. Therefore, if they same two strains emit the same fluorescence, but grow at different rates, the slower growing strain will generate a higher signaling value. When looking at the raw OD_{600} reads at the lowest Mg^{2+} concentration for DK3, DK26, DK136, DF-06, we see that the strains are actively growing and dividing. Therefore, option 2) from above seems like a more probable scenario of what is occurring in these four strains. They are primed to robustly respond at the lowest concentration of Mg^{2+} and have a steep decline in signaling potential at any concentrations higher than that.

5.1.2. The role of O-antigen in PhoPQ response

To find a possible explanation for why our K12 background was our highest signaling strain, we looked for differences in the outer membrane between K12 and our clinical isolates. LPS found on the outer leaflet of the outer membrane in gram negatives has three distinct moieties, 1) an outer membrane embedded lipid A portion, 2) an oligosaccharide core region, and 3) and a highly variable O-antigen region[106,107]. The lipid A portion is widely known as the most conserved and bioactive component within LPS, connecting to the oligosaccharide core. This core can be further divided into a highly conserved inner oligosaccharide region, and an outer oligosaccharide region that connects to the O-antigen[106]. The O-antigen region, which varies greatly in length and density between strains, is not an essential part of LPS and usually not found in *E. coli* K12 due to an insertion sequence (IS) in the *wbbL* gene coding for rhamnosyltransferase, an enzyme critical for O-antigen synthesis[107,108]. We hypothesize that this O-antigen defect in K12 is involved in the higher-fold increase we see in K12 signaling compared to our clinical isolates. In this working model, we believe that the O-antigen of our clinical strains modulates extracellular Mg^{2+} levels, creating a divalent cation microenvironment of its own. As an analogy, the O-antigen serves as 'sponges' that are able to sequester Mg^{2+} ions. Therefore, even in low Mg^{2+} concentrations, the PhoPQ response of these clinical strains are tainted with O-antigen associated divalent cations, thus generating a consistent 2-fold increase for PhoPQ signaling. K12 lacks these 'sponges', therefore response to Mg^{2+} levels reflect Mg^{2+}

concentration within the media. To test this hypothesis, we plan to proceed with two separate experiments. Firstly, we want to conduct ICP analysis to measure a Mg^{2+} coefficient for each strain that measures bacterial cell-associated Mg^{2+} vs. supernatant Mg^{2+} concentrations. We would predict that our clinical isolates will have a higher portion of membrane-associated Mg^{2+} compared to our K12. And secondly, we want to fix the mutated *wbbL* gene in our K12 strain, and test for PhoPQ signaling under the same conditions again. If our hypothesis holds true, we should see a reduction in the fold-change from non-inducing to inducing conditions in our 'fixed' K12 strain.

5.2. PhoPQ signaling as a predictive marker for resistance

We wanted to determine if the altered PhoPQ signaling among our clinical isolates correlated with a phenotypic output. Here, we hypothesized that high PhoPQ signaling strains would have elevated resistance to PMB, a small cationic antimicrobial that targets the negatively charged bacterial cell membrane. We elected to use the *pmrD* signaling as a predictive model for resistance phenotype for three primary reasons: 1) there is no evidence that PMB can be cleaved by OmpT, 2) parallel work in McPhee lab has discovered a novel PhoPQ-independent way that *ompT* is regulated, and 3) the role of *pmrD* in LPS modifications. As mentioned above, PmrD is a connector protein to the PmrAB TCS. This system is widely known as the master regulator of LPS modification, resulting in an overall negative charge on the bacterial membrane. This modification represents a direct mechanism by which bacteria are able to evade killing through PMB.

Results from our PMB resistance screens highlighted several interesting observations. Firstly, strain DK89, the highest *pmrD*, signaling strain, showed highest resistance phenotypes in most of the PMB concentrations tested, supporting our hypothesis. In addition, there was a clear distinction between the strains enhanced ability to resist PMB challenge after being cultured in PhoPQ-inducing vs. repressing media prior to PMB exposure (**Fig. 9d**). We also found evidence of active repression of *pmrD* by PmrB-activated PmrA in strain DK89 (**Fig. 10**). First shown by Kato *et al.* in 2003, PmrB-activated PmrA has shown the ability to directly reduce *pmrD* transcription by binding to the promoter in a repressive manner. When we measured this

phenomenon in our panel of isolates, we found evidence of this negative regulation only in DK89. Therefore, something we plan to do is perform PMB susceptibility assays of DK89 grown in both PhoPQ and PmrAB inducing media (20μM Mg^{2+}, 100μM Fe^{3+}) to see if we can reduce the resistance phenotypes, as suggested by *pmrD* expression levels in Figure 10. The results of the remaining isolates were not what was expected. According to our model, the lowest *pmrD* signaling strain should exhibit the lowest resistance phenotype, and the remaining strains would follow the same sequential pattern. However, this is not what we observed. For example, PP26, a low signaling strain, actually displayed quite high PMB resistance phenotypes among the isolates (**Fig. 10h**). Additionally, we would expect to measure higher PMB resistance when strains were cultured in PhoPQ-inducing vs. repressive media. Strains DK26, DK236 and BW25113 showed elevated PMB resistance when grown in PhoPQ-repressing vs. inducing media, opposite of what we anticipated. This suggests that although PhoPQ-mediated signaling may be necessary for high level resistance to HDPs, it is not sufficient to explain it. To rationalize these results, the remaining portion of this section will discuss these two observations.

5.2.1. Heteroresistance within isogenic cultures causes unusual resistance patterns

Heteroresistance is broadly defined as subpopulations of cells within isogenic cultures that have different susceptibilities to antimicrobials drugs[109,110]. This phenomenon, which is becoming an increasingly prevalent topic in the scientific community, is an ambiguous mechanism where usually susceptible bacteria have subpopulations of antimicrobial resistant cells that can replicate after drug exposure. We wanted to screen our panel of strains to detect if heteroresistant subpopulations were driving the unusual PMB resistance we measured. To do this, we measured *pmrD* activity at the single-cell level using flow cytometry for all our strains grown in either PhoPQ-inducing or repressing media (**Fig. 12**). If *pmrD* transcription varied more in our cells grown in PhoPQ-repressive conditions, where a subpopulation of cells displayed *pmrD* signaling levels higher then when grown in PhoPQ-inducing conditions, it would give us confidence that heteroresistance could be the driving force behind the unusual PMB resistance measured. Strain UM146, a low *pmrD* signaling strain showed significant overlap between of *pmrD* signaling when grown in either PhoPQ-inducing or repressive media (blue dots vs. red dots, **Fig. 12c**). Unfortunately, due the poor growing nature of UM146, we

were unable to perform PMB killing assays on this strain. We were not able to detect significant overlap between the two media-types among the other strains tested. Of note, these single-cell analysis tests were completed using overnight cultures. The sample preparation of our cultures is different than what we do for our PMB resistance screens, where strains are subcultured and grown to mid-log in PhoPQ-inducing or repressing media. Bacteria display different metabolic activity in the different growth phases; therefore, we plan to complete this experiment again, but this time preparing our samples as we would for PMB killing assays. Another separate way we plan to screen for heteroresistant subpopulations within our strains is to plate cultures on nutrient agar plates with set concentrations of PMB, as was demonstrated by Napier *et al.* in 2014. In this screen, cultures would be grown to mid-log, and then be plated on nutrient agar with or without PMB[110]. The frequency of heteroresistant subpopulations would be measured by dividing the number of colonies present on PMB plates by PMB-free plates.

5.2.2. Exploring strain-specific structural PhoQ variation

The PhoQ histidine kinase contains a periplasmic domain (PD) comprised of an α/ß core that senses for divalent cation concentration and the presence of CAMPs[112]. Within this PD are acidic patches that interact with the negatively charged inner membrane phospholipids through divalent cation bridges, with a particularly high affinity for Mg^{2+} ions. When bound to Mg^{2+}, the PD retains a certain conformation that prevents autophosphorylation on C-terminal catalytic domain[112]. Traditionally, it has been thought that CAMPs activate PhoQ by out competing and displacing the Mg^{2+} from the acidic surface on the PD, thus disrupting the divalent cation bridges. However, recent work in 2015 showed evidence of a *Salmonella* PhoQ variant that was impaired for Mg^{2+} sensing but able to respond to CAMPs, suggesting independent recognition mechanisms[111]. This was achieved by mutating the PD through insertion of cysteine residues at positions W104 (located on the α2 helix) and A128 (located on the α4 helix), creating a disulphide bond between the two helices. The structure of the $PhoQ^{W104C\text{-}A128C}$ mutant highly resembled both WT PhoQ PDs from *Salmonella* and *E. coli* backgrounds[111], and in general, *Salmonella* PhoQ PD shares an 80.5% sequence similarity with the *E. coli* PhoQ PD[112]. To test for the virulence of this mutant, the authors infected BALB/c mice with WT *Salmonella,* the $phoQ^{W104C\text{-}A128C}$ strain, and a *ΔphoQ* strain and measured splenic bacterial burden. The $phoQ^{W104C\text{-}A128C}$ mutant had increased bacterial burden compared to mice infected with the

ΔphoQ strain, and exhibited a higher splenic bacterial competitive index compared to the WT strain, highlighting its ability to be a virulent pathogen *in vivo*[111].

We want to examine the PhoPQ sequences from our clinical isolates to screen for possible similar mutations mentioned above. If some of our strains hold a mutation that reduce its ability to respond to Mg^{2+} concentrations while maintaining its capacity to sense cationic peptides like PMB, it would explain why we see high PMB resistance in strains that were low Mg^{2+}-dependent PhoPQ signalers (e.g. for strain PP26, **Fig. 7a, Fig. 10h**). In this circumstance, strains would have a higher propensity to signal through the PhoPQ system after being challenged by PMB rather than induced with Mg^{2+} replete conditions. Therefore, we also plan to measure PhoPQ signaling through our *pmrD*-GFP reporter using a CAMP as a stimulant to determine if we can recapitulate our Mg^{2+} induced results. If the signaling patterns between the two stimuli differ, it would suggest of independent mechanisms of PhoQ sensing in the respective strains.

5.3. Novel insight of conserved signaling systems

Bacteria rely on highly organized signaling through conserved systems to increase their fitness in competitive environments. Here, we have shown the ability of IBDEC strains to differentially signal through the PhoPQ signaling system to survive against antimicrobial threat. Interestingly, we were also able to see the same pattern of differential signaling in two EHEC strains, suggesting that this altered signaling response might exist among strains of other enteric pathogens as well (**Fig. 11**). Recent work from the Coombes showed that AIEC strain NRG857c gains hypermotility and metabolic advantages after mouse colonization, suggesting the adaptive role of these strains *in vivo*[114]. It is possible that our tested strains rapidly and independently evolved across the different gut environments they originally resided in and are now primed to respond a certain way. Due to the known interaction between the host immune system and microbial community in IBD, the signaling and HDP resistance profile of our IBDEC strains could provide insight into the host-specific environment they once colonized.

6. Future Directions

We have two future projects planned that stem from the work uncovered during this thesis project. Firstly, two necessary experiments needed to validate this project directly are: 1) to complete western blots measuring PhoP phosphorylation per strain, and 2) confirm our transcriptional regulation data with qPCR. In the former, we plan to use our PhoP-HA tagged construct in the low copy pWSK129 vector to measure strain-specific PhoP phosphorylation via phos-tag gels. We hope to see the level of PhoP phosphorylation match the level of PhoPQ signaling from our *pmrD* reporter screen. In addition, we plan to use use qPCR on a subset of interesting strains (e.g. DK89) to verify the transcriptional regulation data produced by our *pmrD* reporter screens. Two separate projects will be discussed below.

6.1. Exploring the role of O-antigen

As previously mentioned, there are several planned experiments to look at the role of O-antigen in modulating PhoPQ signaling. ICP analysis of membrane associated Mg^{2+} in BW25113 and our panel of clinical isolates will be completed as an initial screen to determine a strain-specific Mg^{2+} coefficient. In parallel, 'fixing' the broken *wbbL* gene in the K12 background and repeating the *pmrD*-GFP induction assays will give critical insight into the role of O-antigen in PhoPQ signaling. Following the induction assays, PMB resistance screens will be completed to determine if the presence of O-antigen in BW25113 enhances antimicrobial resistance, as suggested in literature[107,113].

6.2. Cloning and sequencing strain-specific PhoPQ

Given the heterogeneity in PhoPQ signaling among IBDEC strains, future projects will attempt to establish a basis for this altered signaling. This will include cloning strain-specific PhoPQ proteins from IBDEC isolates for sequencing and transformation into a ΔphoPQ K12 strain. The sequencing results will be analyzed for potential important mutations. Further, the various strain-specific PhoPQ proteins in a ΔphoPQ K12 background will be screened by completing *pmrD*-GFP induction assays to determine if the signaling heterogeneity is a product

of these two proteins, or from accessory genes feeding back into the system. If the PhoPQ proteins themselves are the sole reason behind the heterogenous signaling, then the signaling from these experiments would match previous signaling data (**Fig. 7a**). If not, it gives as solid evidence of accessory genes involved in the altered signaling levels among strains.

References:

1. Erb, A., et al. Prevalence of Antibiotic Resistance in Escherichia Coli: Overview of Geographical, Temporal, and Methodological Variations. *Eur J Clin Microbiol Infect Dis*, 2007, doi:10.1007/s10096-006-0248-2.
2. Rasko, David A., et al. "The Pangenome Structure of Escherichia Coli: Comparative Genomic Analysis of E. Coli Commensal and Pathogenic Isolates." *Journal of Bacteriology*, vol. 190, no. 20, American Society for Microbiology, Oct. 2008, pp. 6881–93, doi:10.1128/JB.00619-08.
3. Goldfine, H. "Bacterial Membranes and Lipid Packing Theory." *Journal of Lipid Research*, vol. 25, no. 13, 1984, pp. 1501–07, http://www.ncbi.nlm.nih.gov/pubmed/6530599.
4. Tlaskalová-Hogenová, Helena, et al. "The Role of Gut Microbiota (Commensal Bacteria) and the Mucosal Barrier in the Pathogenesis of Inflammatory and Autoimmune Diseases and Cancer: Contribution of Germ-Free and Gnotobiotic Animal Models of Human Diseases." *Cellular & Molecular Immunology*, vol. 867, no. 10, 2011, pp. 110–20, doi:10.1038/cmi.2010.67.
5. Kostic, Aleksandar D., et al. *The Microbiome in Inflammatory Bowel Diseases: Current Status and the Future Ahead*. doi:10.1053/j.gastro.2014.02.009. Accessed 10 May 2018.
6. Conway, Tyrrell, and Paul S. Cohen. *Commensal and Pathogenic Escherichia Coli Metabolism in the Gut*. doi:10.1128/microbiolspec.MBP-0006-2014. Accessed 10 May 2018.
7. Rocchi Msc, Angela, et al. "Inflammatory Bowel Disease: A Canadian Burden of Illness Review." *Can J Gastroenterol*, vol. 26, no. 11, 2012, https://www.ncbi.nlm.nih.gov/pmc/articles/PMC3495699/pdf/cjg26811.pdf.
8. *Ulcerative Colitis - Crohn's and Colitis Canada*. http://www.crohnsandcolitis.ca/About-Crohn-s-Colitis/What-are-Crohns-and-Colitis/ulcerative-colitis?gclid=Cj0KCQjwodrXBRCzARIsAIU59TIi0Yaoc1uw2zq7TuQw0qZmSvRCBsgGNB1DtyhjcXkwPbEsBXHW9RsaAr9OEALw_wcB. Accessed 12 May 2018.
9. Gecse, Krisztina B., and Péter L. Lakatos. "Biologicals and Biosimilars in IBD — the Road to Personalized Treatment." *Nature Reviews Gastroenterology & Hepatology*, vol. 14, no. 2, Nature Publishing Group, Feb. 2017, pp. 74–76, doi:10.1038/nrgastro.2016.206.
10. Louis, Edouard. "Stopping Biologics in IBD—What Is the Evidence?" *Inflamm Bowel Dis*, vol. 24, no. 4, 2018, https://academic.oup.com/ibdjournal/article-abstract/24/4/725/4934202.
11. Kaplan, Gilaad G. "The Global Burden of IBD from 2015 to 2025 Nature Reviews Gastroenterology & Hepatology Nature Publishing Group." *Nature Publishing Group*, vol. 12, no. 12, 2015, pp. 720–27, https://www.nature.com/articles/nrgastro.2015.150.
12. Frolkis, Alexandra, et al. "Environment and the Inflammatory Bowel Diseases." *Canadian Journal of Gastroenterology*, vol. 27, no. 3, Hindawi, 2013, pp. e18–24, doi:10.1155/2013/102859.
13. Molodecky, Natalie A., et al. "Increasing Incidence and Prevalence of the Inflammatory Bowel Diseases With Time, Based on Systematic Review." *YGAST*, vol. 142, 2012, pp. 46-54.e42, doi:10.1053/j.gastro.2011.10.001.
14. Calkins, Beverly M. "A Meta-Analysis of the Role of Smoking in Inflammatory Bowel Disease." *Digestive Diseases and Sciences*, vol. 34, no. 12, Kluwer Academic Publishers-Plenum Publishers, Dec. 1989, pp. 1841–54, doi:10.1007/BF01536701.
15. Harries, A. D., et al. "Non-Smoking: A Feature of Ulcerative Colitis." *British Medical Journal (Clinical Research Ed.)*, vol. 284, no. 6317, 1982, p. 706, http://www.ncbi.nlm.nih.gov/pubmed/6802296%0Ahttp://www.pubmedcentral.nih.gov/articlerender.fcgi?artid=PMC1496690.

16. Stagg, Andrew J., et al. “Smokers with Active Crohn’s Disease Have a Clinically Relevant Dysbiosis of the Gastrointestinal Microbiota*.” *Inflammatory Bowel Diseases*, vol. 18, no. 6, 2011, pp. 1092–100, doi:10.1002/ibd.21864.
17. Boyko, Edward J., et al. “Risk of Ulcerative Colitis among Former and Current Cigarette Smokers.” *New England Journal of Medicine*, vol. 316, no. 12, Mar. 1987, pp. 707–10, doi:10.1056/NEJM198703193161202.
18. Xavier, RJ, et al. “Unravelling the Pathogenesis of Inflammatory Bowel Disease R. J. Xavier1,2& D. K. Podolsky1.” *Nature.Com*, http://immunologie.charite.de/fileadmin/user_upload/microsites/m_cc12/immunologie/Lehre/review-IBD-nature.pdf. Accessed 15 May 2018.
19. Jostins, Luke, et al. “Host-Microbe Interactions Have Shaped the Genetic Architecture of Inflammatory Bowel Disease.” *Nature*, vol. 491, no. 7422, NIH Public Access, Nov. 2012, pp. 119–24, doi:10.1038/nature11582.
20. Ogura, Yasunori, et al. “A Frameshift Mutation in NOD2 Associated with Susceptibility to Crohn’s Disease1. Ogura Y, Bonen DK, Inohara N, et Al. A Frameshift Mutation in NOD2 Associated with Susceptibility to Crohn’s Disease. Nature. 2001;411(6837):603-606. Doi:10.1038/35079114.” *Nature*, vol. 411, no. 6837, 2001, pp. 603–06, doi:10.1038/35079114.
21. Pidasheva, Svetlana, et al. “Functional Studies on the IBD Susceptibility Gene IL23R Implicate Reduced Receptor Function in the Protective Genetic Variant R381Q.” *PLoS ONE*, edited by Sunil K. Ahuja, vol. 6, no. 10, Public Library of Science, Oct. 2011, p. e25038, doi:10.1371/journal.pone.0025038.
22. Cummings, Fraser J. R., et al. “Confirmation of the Role of ATG16l1 as a Crohn’s Disease Susceptibility Gene.” *Inflammatory Bowel Diseases*, vol. 13, no. 8, Aug. 2007, pp. 941–46, doi:10.1002/ibd.20162.
23. Weersma, Rinse K., et al. “ATG16L1 and IL23R Are Associated With Inflammatory Bowel Diseases but Not With Celiac Disease in The Netherlands.” *American Journal of Gastroenterology*, 2008, doi:10.1111/j.1572-0241.2007.01660.x.
24. Hampe, Jochen, et al. “A Genome-Wide Association Scan of Nonsynonymous SNPs Identifies a Susceptibility Variant for Crohn Disease in ATG16L1.” *Nature Genetics*, vol. 39, no. 2, 2007, pp. 207–11, doi:10.1038/ng1954.
25. Fava, Francesca, and Silvio Danese. “Intestinal Microbiota in Inflammatory Bowel Disease: Friend of Foe?” *World Journal of Gastroenterology*, vol. 17, no. 5, Baishideng Publishing Group Inc, Feb. 2011, pp. 557–66, doi:10.3748/wjg.v17.i5.557.
26. Frank, Daniel N., et al. “Disease Phenotype and Genotype Are Associated with Shifts in Intestinal-Associated Microbiota in Inflammatory Bowel Diseases.” *Inflammatory Bowel Diseases*, vol. 17, no. 1, NIH Public Access, Jan. 2011, pp. 179–84, doi:10.1002/ibd.21339.
27. Gevers, Dirk, et al. “The Treatment-Naive Microbiome in New-Onset Crohn’s Disease.” *Cell Host & Microbe*, vol. 15, no. 3, Cell Press, Mar. 2014, pp. 382–92, doi:10.1016/J.CHOM.2014.02.005.
28. Darfeuille-Michaud, Arlette, et al. “High Prevalence of Adherent-Invasive Escherichia Coli Associated with Ileal Mucosa in Crohn’s Disease.” *Gastroenterology*, vol. 127, no. 2, Elsevier, Aug. 2004, pp. 412–21, doi:10.1053/j.gastro.2004.04.061.
29. Darfeuille-Michaud, A., et al. “Presence of Adherent Escherichia Coli Strains in Ileal Mucosa of Patients with Crohn’s Disease.” *Gastroenterology*, vol. 115, no. 6, 1998, pp. 1405–13, doi:10.1016/S0016-5085(98)70019-8.

30. Carvalho, Frédéric A., et al. “Crohn’s Disease Adherent-Invasive Escherichia Coli Colonize and Induce Strong Gut Inflammation in Transgenic Mice Expressing Human CEACAM.” *The Journal of Experimental Medicine*, vol. 206, no. 10, Rockefeller University Press, Sept. 2009, pp. 2179–89, doi:10.1084/jem.20090741.
31. Barnich, Nicolas, et al. “CEACAM6 Acts as a Receptor for Adherent-Invasive E. Coli, Supporting Ileal Mucosa Colonization in Crohn Disease.” *The Journal of Clinical Investigation*, vol. 117, no. 6, American Society for Clinical Investigation, June 2007, pp. 1566–74, doi:10.1172/JCI30504.
32. Small, Cherrie-Lee N., et al. “Persistent Infection with Crohn’s Disease-Associated Adherent-Invasive Escherichia Coli Leads to Chronic Inflammation and Intestinal Fibrosis.” *Nature Communications*, vol. 4, Nature Publishing Group, June 2013, p. 1957, doi:10.1038/ncomms2957.
33. Hancock, Robert E. W., and Hans Georg Sahl. “Antimicrobial and Host-Defense Peptides as New Anti-Infective Therapeutic Strategies.” *Nature Biotechnology*, vol. 24, no. 12, 2006, pp. 1551–57, doi:10.1038/nbt1267.
34. Brodgen KA. “Antimicrobial Peptides: Pore Formers or Metabolic Inhibitors in Bacteria?” *Nature Reviews. Microbiology*, vol. 3, no. 3, 2005, pp. 238–50, doi:10.1038/nrmicro1098.
35. Hancock, R. E., and M. G. Scott. “The Role of Antimicrobial Peptides in Animal Defenses.” *Proceedings of the National Academy of Sciences of the United States of America*, vol. 97, no. 16, 2000, pp. 8856–61, http://www.ncbi.nlm.nih.gov/pubmed/10922046%0Ahttp://www.pubmedcentral.nih.gov/articlerender.fcgi?artid=PMC34023.
36. Hancock, Robert E. W., et al. “The Immunology of Host Defence Peptides: Beyond Antimicrobial Activity.” *Nature Reviews Immunology*, vol. 16, no. 5, 2016, pp. 321–34, doi:10.1038/nri.2016.29.
37. Beier, Dagmar, and Roy Gross. “Regulation of Bacterial Virulence by Two-Component Systems.” *Current Opinion in Microbiology*, vol. 9, no. 2, 2006, pp. 143–52, doi:10.1016/j.mib.2006.01.005.
38. Breland, Erin J., et al. “An Overview of Two-Component Signal Transduction Systems Implicated in Extra-Intestinal Pathogenic E. Coli Infections.” *Frontiers in Cellular and Infection Microbiology*, vol. 7, May 2017, doi:10.3389/fcimb.2017.00162.
39. Dalebroux, Zachary D., and Samuel I. Miller. “Salmonellae PhoPQ Regulation of the Outer Membrane to Resist Innate Immunity.” *Current Opinion in Microbiology*, vol. 17, NIH Public Access, Feb. 2014, pp. 106–13, doi:10.1016/j.mib.2013.12.005.
40. Hwang, Peter M., et al. “Solution Structure and Dynamics of the Outer Membrane Enzyme PagP by NMR.” *Proceedings of the National Academy of Sciences of the United States of America*, vol. 99, no. 21, National Academy of Sciences, Oct. 2002, pp. 13560–65, doi:10.1073/pnas.212344499.
41. Rubin, Erica J., et al. “PmrD Is Required for Modifications to Escherichia Coli Endotoxin That Promote Antimicrobial Resistance.” *Antimicrobial Agents and Chemotherapy*, vol. 59, no. 4, American Society for Microbiology, Apr. 2015, pp. 2051–61, doi:10.1128/AAC.05052-14.
42. Schurek, Kristen N., et al. “Involvement of PmrAB and PhoPQ in Polymyxin B Adaptation and Inducible Resistance in Non-Cystic Fibrosis Clinical Isolates of Pseudomonas Aeruginosa.” *Antimicrobial Agents and Chemotherapy*, vol. 53, no. 10, American Society for Microbiology, Oct. 2009, pp. 4345–51, doi:10.1128/AAC.01267-08.

43. Farizano, Juan V, et al. “The PmrAB System-Inducing Conditions Control Both Lipid A Remodeling and O-Antigen Length Distribution, Influencing the Salmonella Typhimurium-Host Interactions.” *The Journal of Biological Chemistry*, vol. 287, no. 46, American Society for Biochemistry and Molecular Biology, Nov. 2012, pp. 38778–89, doi:10.1074/jbc.M112.397414.
44. Blount, Zachary D. “The Unexhausted Potential of E. Coli.” *ELife*, vol. 4, eLife Sciences Publications, Ltd, Mar. 2015, doi:10.7554/eLife.05826.
45. Randal Bollinger, R., et al. “Human Secretory Immunoglobulin A May Contribute to Biofilm Formation in the Gut.” *Immunology*, vol. 109, no. 4, Wiley/Blackwell (10.1111), Aug. 2003, pp. 580–87, doi:10.1046/j.1365-2567.2003.01700.x.
46. Murthy, Aditya, et al. “A Crohn’s Disease Variant in Atg16l1 Enhances Its Degradation by Caspase 3.” *Nature*, vol. 506, no. 7489, Feb. 2014, pp. 456–62, doi:10.1038/nature13044.
47. McPhee, Joseph B., et al. “Host Defense Peptide Resistance Contributes to Colonization and Maximal Intestinal Pathology by Crohn’s Disease-Associated Adherent-Invasive Escherichia Coli.” *Infection and Immunity*, vol. 82, no. 8, American Society for Microbiology, Aug. 2014, pp. 3383–93, doi:10.1128/IAI.01888-14.
48. Thomassin, Jenny-Lee, et al. “OmpT Outer Membrane Proteases of Enterohemorrhagic and Enteropathogenic Escherichia Coli Contribute Differently to the Degradation of Human LL-37.” *Infection and Immunity*, vol. 80, no. 2, American Society for Microbiology, Feb. 2012, pp. 483–92, doi:10.1128/IAI.05674-11.
49. Capra, Emily J., and Michael T. Laub. “Evolution of Two-Component Signal Transduction Systems.” *Annual Review of Microbiology*, vol. 66, no. 1, Oct. 2012, pp. 325–47, doi:10.1146/annurev-micro-092611-150039.
50. Casino, et al. “The Mechanism of Signal Transduction by Two-Component Systems.” *Current Opinion in Structural Biology*, vol. 20, no. 6, 2010, pp. 763–71, doi:10.1016/j.sbi.2010.09.010.
51. Gao, Rong, and Ann M. Stock. “Biological Insights from Structures of Two-Component Proteins.” *Annual Review of Microbiology*, vol. 63, no. 1, Oct. 2009, pp. 133–54, doi:10.1146/annurev.micro.091208.073214.
52. He, Xiaoyuan, and Shuishu Wang. “DNA Consensus Sequence Motif for Binding Response Regulator PhoP, a Virulence Regulator of Mycobacterium Tuberculosis.” *Biochemistry*, vol. 53, no. 51, 2014, pp. 8008–20, doi:10.1021/bi501019u.
53. Goulian, Mark. “Two-Component Signaling Circuit Structure and Properties.” *Current Opinion in Microbiology*, vol. 13, no. 2, 2010, pp. 184–89, doi:10.1016/j.mib.2010.01.009.
54. Russo, Frank D., and Thomas J. Silhavy. “The Essential Tension: Opposed Reactions in Bacterial Two-Component Regulatory Systems.” *Trends in Microbiology*, vol. 1, no. 8, 1 Nov. 1993, pp. 306–10, doi:10.1016/0966-842X(93)90007-E.
55. Batchelor, E., and M. Goulian. “Robustness and the Cycle of Phosphorylation and Dephosphorylation in a Two-Component Regulatory System.” *Proceedings of the National Academy of Sciences*, vol. 100, no. 2, 2003, pp. 691–96, doi:10.1073/pnas.0234782100.
56. Miyashiro, T., and M. Goulian. “High Stimulus Unmasks Positive Feedback in an Autoregulated Bacterial Signaling Circuit.” *Proceedings of the National Academy of Sciences*, vol. 105, no. 45, 2008, pp. 17457–62, doi:10.1073/pnas.0807278105.
57. Lippa, Andrew M., and Mark Goulian. “Feedback Inhibition in the PhoQ/PhoP Signaling System by a Membrane Peptide.” *PLoS Genetics*, vol. 5, no. 12, 2009, p. 1000788, doi:10.1371/journal.pgen.1000788.

58. Lippa, Andrew M., and Mark Goulian. “Perturbation of the Oxidizing Environment of the Periplasm Stimulates the PhoQ/PhoP System in Escherichia Coli.” *Journal of Bacteriology*, vol. 194, no. 6, 2012, pp. 1457–63, doi:10.1128/JB.06055-11.
59. Herrera, Carmen M., et al. “Activation of PmrA Inhibits LpxT-Dependent Phosphorylation of Lipid A Promoting Resistance to Antimicrobial Peptides.” *Molecular Microbiology*, vol. 76, no. 6, 2010, pp. 1444–60, doi:10.1111/j.1365-2958.2010.07150.x.
60. Bader, Martin W., et al. “Recognition of Antimicrobial Peptides by a Bacterial Sensor Kinase.” *Cell*, vol. 122, no. 3, 2005, pp. 461–72, doi:10.1016/j.cell.2005.05.030.
61. Girardin, Stephen E., et al. “Nod2 Is a General Sensor of Peptidoglycan through Muramyl Dipeptide (MDP) Detection.” *Journal of Biological Chemistry*, vol. 278, no. 11, American Society for Biochemistry and Molecular Biology, Mar. 2003, pp. 8869–72, doi:10.1074/jbc.C200651200.
62. Cadwell, Ken, et al. “Virus-Plus-Susceptibility Gene Interaction Determines Crohn’s Disease Gene Atg16L1 Phenotypes in Intestine.” *Cell*, vol. 141, no. 7, NIH Public Access, June 2010, pp. 1135–45, doi:10.1016/j.cell.2010.05.009.
63. Cadwell, Ken, et al. “A Key Role for Autophagy and the Autophagy Gene Atg16l1 in Mouse and Human Intestinal Paneth Cells.” *Nature*, vol. 456, no. 7219, NIH Public Access, Nov. 2008, pp. 259–63, doi:10.1038/nature07416.
64. Elhenawy, Wael, et al. “A Polymicrobial View of Disease Potential in Crohn’s-Associated Adherent-Invasive E. Coli.” *Gut Microbes*, vol. 9, no. 2, Taylor & Francis, 4 Mar. 2017, pp. 1–9, doi:10.1080/19490976.2017.1378291.
65. Kato, A., et al. “Closing the Loop: The PmrA/PmrB Two-Component System Negatively Controls Expression of Its Posttranscriptional Activator PmrD.” *Proceedings of the National Academy of Sciences*, vol. 100, no. 8, 2003, pp. 4706–11, doi:10.1073/pnas.0836837100.
66. El-Halfawy, Omar M., and Miguel A. Valvano. “Antimicrobial Heteroresistance: An Emerging Field in Need of Clarity.” *Clinical Microbiology Reviews*, vol. 28, no. 1, 2015, pp. 191–207, doi:10.1128/CMR.00058-14.
67. Ricciuto, Amanda, et al. “Diagnostic Delay in Canadian Children with Inflammatory Bowel Disease Is More Common in Crohn’s Disease and Associated with Decreased Height.” *Archives of Disease in Childhood*, vol. 103, no. 4, 2018, pp. 319–26, doi:10.1136/archdischild-2017-313060.
68. Benchimol, Eric I., et al. “Changing Age Demographics of Inflammatory Bowel Disease in Ontario, Canada.” *Inflammatory Bowel Diseases*, vol. 20, no. 10, 2014, pp. 1761–69, doi:10.1097/mib.0000000000000103.
69. Benchimol, E. I., et al. “Increasing Incidence of Paediatric Inflammatory Bowel Disease in Ontario, Canada: Evidence from Health Administrative Data.” *Gut,* vol. 58, 2009, pp. 1490–97, doi:10.1136/gut.2009.188383.
70. N., Gupta, et al. “Presentation and Disease Course in Early- Compared to Later-Onset Pediatric Crohn’s Disease.” *American Journal of Gastroenterology*, vol. 103, no. 8, 2008, pp. 2092–98, https://www.nature.com/articles/ajg2008407.
71. De Ridder, Lissy, et al. “Genetic Susceptibility Has a More Important Role in Pediatric-Onset Crohn’s Disease than in Adult-Onset Crohn’s Disease.” *Inflammatory Bowel Diseases*, vol. 13, no. 9, Sept. 2007, pp. 1083–92, doi:10.1002/ibd.20171.
72. Iida, Tomoya, et al. “Impact of Autophagy of Innate Immune Cells on Inflammatory Bowel Disease.” *Cells*, vol. 8, no. 1, 2018, p. 7, doi:10.3390/cells8010007.

73. Plantinga, Theo S., et al. “Crohn’s Disease-Associated ATG16L1 Polymorphism Modulates pro-Inflammatory Cytokine Responses Selectively upon Activation of NOD2.” *Gut*, vol. 60, no. 9, 2011, pp. 1229–35, doi:10.1136/gut.2010.228908.
74. Baümler, Andreas J., and Vanessa Sperandio. “Interactions between the Microbiota and Pathogenic Bacteria in the Gut.” *Nature*, vol. 535, no. 7610, NIH Public Access, 2016, pp. 85–93, doi:10.1038/nature18849.
75. Keeney, Kristie M., and B. Brett Finlay. “Enteric Pathogen Exploitation of the Microbiota-Generated Nutrient Environment of the Gut.” *Current Opinion in Microbiology*, vol. 14, no. 1, NIH Public Access, Feb. 2011, pp. 92–98, doi:10.1016/j.mib.2010.12.012.
76. Stecher, Bärbel. “The Roles of Inflammation, Nutrient Availability and the Commensal Microbiota in Enteric Pathogen Infection.” Metabolism and Bacterial Pathogenesis, vol. 3, no. 3, *American Society of Microbiology*, 2015, pp. 297–320, doi:10.1128/microbiolspec.mbp-0008-2014.
77. Peschel, A., et al. “The Co-Evolution of Host Cationic Antimicrobial Peptides and Microbial Resi...: University of Liverpool Library.” *Nature.Com*, https://www.nature.com/articles/nrmicro1441. Accessed 20 June 2019.
78. Netea-Maier, Romana T., et al. “Modulation of Inflammation by Autophagy: Consequences for Human Disease.” *Autophagy*, vol. 12, no. 2, 2016, pp. 245–60, doi:10.1080/15548627.2015.1071759.
79. Conway, Tyrrell, and Paul S. Cohen. “Commensal and Pathogenic Escherichia Coli Metabolism in the Gut.” *Microbiology Spectrum*, vol. 3, no. 3, NIH Public Access, June 2015, doi:10.1128/microbiolspec.mbp-0006-2014.
80. Matic, I., et al. “Highly Variable Mutation Rates in Commensal and Pathogenic Escherichia Coli.” *Science*, vol. 277, no. 5333, 1997, pp. 1833–34, doi:10.1126/science.277.5333.1833.
81. Tenaillon, Olivier, et al. “The Population Genetics of Commensal Escherichia Coli.” *Nature Reviews Microbiology*, vol. 8, no. 3, 2010, pp. 207–17, doi:10.1038/nrmicro2298.
82. Rasko, David A., et al. “The Pangenome Structure of Escherichia Coli: Comparative Genomic Analysis of E. Coli Commensal and Pathogenic Isolates.” *Journal of Bacteriology*, vol. 190, no. 20, 2008, pp. 6881–93, doi:10.1128/JB.00619-08.
83. McDaniel, T. K., et al. “A Genetic Locus of Enterocyte Effacement Conserved among Diverse Enterobacterial Pathogens.” *Proceedings of the National Academy of Sciences*, vol. 92, no. 5, 2006, pp. 1664–68, doi:10.1073/pnas.92.5.1664.
84. Cepeda-Molero, Massiel, et al. “Attaching and Effacing (A/E) Lesion Formation by Enteropathogenic E. Coli on Human Intestinal Mucosa Is Dependent on Non-LEE Effectors.” *PLoS Pathogens*, edited by Brian K. Coombes, vol. 13, no. 10, Oct. 2017, p. e1006706, doi:10.1371/journal.ppat.1006706.
85. Franzin, Fernanda M., and Marcelo P. Sircili. “Locus of Enterocyte Effacement: A Pathogenicity Island Involved in the Virulence of Enteropathogenic and Enterohemorragic Escherichia Coli Subjected to a Complex Network of Gene Regulation.” *BioMed Research International*, vol. 2015, Hindawi Limited, 2015, pp. 1–10, doi:10.1155/2015/534738.
86. Snyder, Jennifer A., et al. “Transcriptome of Uropathogenic Escherichia Coli during Urinary Tract Infection.” *Infection and Immunity*, vol. 72, no. 11, 2004, pp. 6373–81, doi:10.1128/IAI.72.11.6373-6381.2004.
87. Tabaqchali, S., et al. “Escherichia Coli Antibodies in Patients with Inflammatory Bowel Disease.” *Gut*, vol. 19, no. 2, 1978, pp. 108–13, doi:10.1136/gut.19.2.108.

88. J., Boudeau, et al. “Invasive Ability of an Escherichia Coli Strain Isolated from the Ileal Mucosa of a Patient with Crohn’s Disease.” *Infection and Immunity*, vol. 67, no. 9, 1999, pp. 4499–509, https://iai.asm.org/content/67/9/4499.short.
89. Boudeau, Jérôme, et al. “Type 1 Pili-Mediated Adherence of Escherichia Coli Strain LF82 Isolated from Crohn’s Disease Is Involved in Bacterial Invasion of Intestinal Epithelial Cells.” *Molecular Microbiology*, vol. 39, no. 5, Feb. 2001, pp. 1272–84, doi:10.1046/j.1365-2958.2001.02315.x.
90. Glasser, A. L., et al. “Adherent Invasive Escherichia Coli Strains from Patients with Crohn’s Disease Survive and Replicate within Macrophages without Inducing Host Cell Death.” *Infection and Immunity*, vol. 69, no. 9, 2001, pp. 5529–37, https://iai.asm.org/content/69/9/5529.short.
91. Delmas, Julien, et al. “Metabolic Adaptation of Adherent-Invasive Escherichia Coli to Exposure to Bile Salts.” *Scientific Reports*, vol. 9, no. 1, 2019, doi:10.1038/s41598-019-38628-1.
92. Shaler, Christopher R., et al. “The Unique Lifestyle of Crohn’s Disease-Associated Adherent-Invasive Escherichia Coli.” *Journal of Molecular Biology*, 2019, doi:10.1016/j.jmb.2019.04.023.
93. Dogan, Belgin, et al. “Inflammation-Associated Adherent-Invasive Escherichia Coli Are Enriched in Pathways for Use of Propanediol and Iron and M-Cell Translocation.” *Inflammatory Bowel Diseases*, vol. 20, no. 11, Narnia, Nov. 2014, pp. 1919–32, doi:10.1097/MIB.0000000000000183.
94. Carvalho, Frédéric A., et al. “Crohn’s Disease Adherent-Invasive Escherichia Coli Colonize and Induce Strong Gut Inflammation in Transgenic Mice Expressing Human CEACAM.” *The Journal of Experimental Medicine*, vol. 206, no. 10, 2009, pp. 2179–89, doi:10.1084/jem.20090741.
95. Mookherjee, N., and R. E. W. Hancock. “Cationic Host Defence Peptides: Innate Immune Regulatory Peptides as a Novel Approach for Treating Infections.” *Cellular and Molecular Life Sciences*, vol. 64, no. 7–8, 19 Apr. 2007, pp. 922–33, doi:10.1007/s00018-007-6475-6.
96. Bevins, C. I., et al. “Defensins and Innate Host Defence of the Gastrointestinal Tract.” *Gut*, vol. 45, no. 6, 1999, pp. 911–15, doi:10.1136/gut.45.6.911.
97. De Smet, Kris, and Roland Contreras. “Human Antimicrobial Peptides: Defensins, Cathelicidins and Histatins.” *Biotechnology Letters*, vol. 27, no. 18, Sept. 2005, pp. 1337–47, doi:10.1007/s10529-005-0936-5.
98. J.P., Meisch, et al. “Human -Defensin 3 Peptide Is Increased and Redistributed in Crohn’s Ileitis.” *Inflammatory Bowel Diseases*, vol. 19, no. 5, 2013, pp. 942–53, https://academic.oup.com/ibdjournal/article-abstract/19/5/942/4603083.
99. Schauber, Jürgen, et al. “Heterogeneous Expression of Human Cathelicidin HCAP18/LL-37 in Inflammatory Bowel Diseases.” *European Journal of Gastroenterology and Hepatology*, vol. 18, no. 6, 2006, pp. 615–21, doi:10.1097/00042737-200606000-00007.
100. Jin, T., et al. “Staphylococcus Aureus Resists Human Defensins by Production of Staphylokinase, a Novel Bacterial Evasion Mechanism.” *The Journal of Immunology*, vol. 172, no. 2, 2014, pp. 1169–76, doi:10.4049/jimmunol.172.2.1169.
101. Ernst, Robert K., et al. “Salmonella Typhimurium Outer Membrane Remodeling: Role in Resistance to Host Innate Immunity.” *Microbes and Infection*, vol. 3, no. 14–15, 2001, pp. 1327–34, doi:10.1016/S1286-4579(01)01494-0.
102. McPhee, Joseph B., et al. “Cationic Antimicrobial Peptides Activate a Two-Component Regulatory System, PmrA-PmrB, That Regulates Resistance to Polymyxin B and Cationic

Antimicrobial Peptides in Pseudomonas Aeruginosa." *Molecular Microbiology*, vol. 50, no. 1, Aug. 2003, pp. 205–17, doi:10.1046/j.1365-2958.2003.03673.x.
103. Peschel, Andreas. "How Do Bacteria Resist Human Antimicrobial Peptides?" *Trends in Microbiology*, vol. 10, no. 4, 2002, pp. 179–86, doi:10.1016/S0966-842X(02)02333-8.
104. Guina, Tina, et al. "A PhoP-Regulated Outer Membrane Protease of Salmonella Enterica Serovar Typhimurium Promotes Resistance to Alpha-Helical Antimicrobial Peptides." *Journal of Bacteriology*, vol. 182, no. 14, 2000, pp. 4077–86, doi:10.1128/JB.182.14.4077-4086.2000.
105. Bren, Anat, et al. "A Comprehensive Library of Fluorescent Transcriptional Reporters for Escherichia Coli." *Nature Methods*, vol. 3, no. 8, 2006, pp. 623–28, doi:10.1038/nmeth895.
106. Meredith, Timothy C., et al. "Redefining the Requisite Lipopolysaccharide Structure in Escherichia Coli." *ACS Chemical Biology*, vol. 1, no. 1, 2006, pp. 33–42, doi:10.1021/cb0500015.
107. Sharp, Connor, et al. "O-Antigen-Dependent Colicin Insensitivity of Uropathogenic Escherichia Coli." *Journal of Bacteriology*, vol. 201, no. 4, 2019, doi:10.1128/JB.00545-18.
108. G., Stevenson, et al. "Structure of the O Antigen of Escherichia Coli K-12 and the Sequence of Its Rfb Gene Cluster." *Journal of Bacteriology*, vol. 176, no. 13, 1994, pp. 4144–56, https://jb.asm.org/content/176/13/4144.short.
109. Band, Victor I., and David S. Weiss. "Heteroresistance: A Cause of Unexplained Antibiotic Treatment Failure?" *PLOS Pathogens*, edited by Jorn Coers, vol. 15, no. 6, June 2019, p. e1007726, doi:10.1371/journal.ppat.1007726.
110. Napier, Brooke A., et al. "Colistin Heteroresistance in Enterobacter Cloacae Is Associated with Cross-Resistance to the Host Antimicrobial Lysozyme." *Antimicrobial Agents and Chemotherapy,* vol. 58, no. 9, 2014, pp. 5594–97, doi:10.1128/aac.02432-14.
111. Hicks, Kevin G., et al. "Acidic PH and Divalent Cation Sensing by PhoQ Are Dispensable for Systemic Salmonellae Virulence." *ELife,* vol. 4, no. MAY, 2015, pp. 1–59, doi:10.7554/eLife.06792.
112. Cho, Uhn Soo, et al. "Metal Bridges between the PhoQ Sensor Domain and the Membrane Regulate Transmembrane Signaling." *Journal of Molecular Biology*, vol. 356, no. 5, 2006, pp. 1193–206, doi:10.1016/j.jmb.2005.12.032.
113. Allen, Chris A., et al. "Transposon-Derived Brucella Abortus Rough Mutants Are Attenuated and Exhibit Reduced Intracellular Survival." *Infection and Immunity*, vol. 66, no. 3, 1998, pp. 1008–16, http://iai.asm.org/.
114. Elhenawy, Wael, et al. "Host-Specific Adaptive Diversification of Crohn's Disease-Associated Adherent-Invasive Escherichia Coli." *Cell Host and Microbe*, vol. 25, no. 2, 2019, pp. 301-312.e5, doi:10.1016/j.chom.2018.12.010.
115. Kus, Julianne V, et al. "Bile Salts Induce Resistance to Polymyxin in Enterohemorrhagic Escherichia Coli O157:H7." *Journal of Bacteriology*, vol. 193, no. 17, 2011, pp. 4509–15, doi:10.1128/JB.00200-11.